PHYSICAL SOCIETY

MEMOIRS

OF THE

COLLEGE OF SCIENCE

KYOTO IMPERIAL UNIVERSITY

SERIES A

VOL. XIX, NO. 2

MARCH 1936

KYOTO

Anomalous Deflection of Seismic Rays in Volcanic Districts

(Part III of the Geophysical Studies on the Volcano Aso)

By **Kenzô Sassa**

(Received October 20, 1935)

1. Introduction

Soon after the beginning of seismographic observations at the Beppu Geophysical Laboratory in 1926, it came to my attention that azimuths of recorded initial motions of earthquakes in the Kumamoto and Aso districts extending over to the southwest of the observatory were deviated greatly to the south from their epicentral azimuths. At first it was suspected that the discrepancies between the two azimuths were due to some instrumental defects, but it was not very long before I came to the opinion that the cause of the discrepancies should be sought in the geological structure of the upper crust of the volcanic district. Three years later, in 1929, another set of Wiechert seismographs of the same type as that at the Beppu Geophysical Laboratory was installed at the Aso Volcanological Laboratory then newly completed, and similar lateral deflections of seismic rays were also observed there, in accordance with my expectation. The observational data of the two stations having now accumulated sufficiently to throw some light upon the anomalous structure of the upper crust in the two volcanic districts, a preliminary report will be given in the following pages.

2. Instruments

At the Geophysical Laboratory at Beppu, the instruments used were

	T_0	v_0	V
Wiechert horizontal comp. seismograph	12.0 sec.	4 : 1	200
Wiechert vertical comp. seismograph	4.6	4 : 1	150
Omori portable tremor recorder	4.0	no damper	40

the last mentioned being used as an auxiliary instrument, for a short period from Dec. 1931 to July 1932. At the Aso Volcanological

Laboratory the instruments were those described in the preceding paper, Part I[1], and have the following constants.

	T_0	v_0	T_1	v_1	k	V
	sec.		sec.			
Wiechert horizontal comp. seismograph	10.0	4 : 1				200
Wiechert vertical comp. seismograph	4.6	4 : 1				150
Micro - seismographs, G_A horizontal comp.	8.0	just aperiodic	4.0	just aperiodic	627	2800
Micro - seismograph, G_A vertical comp.	8.0	just aperiodic	4.0	just aperiodic	1975	2800

The micro-seismographs, G_A were only used for about eight hours every day in order to observe originally volcanic micro-tremors of the second kind for the two years 1932 and 1933, and the number of earthquakes recorded by them was therefore only 11, with the exception of the volcanic earthquakes occurring in the district of Aso, but they served to ascertain whether the instrumental errors of the observed epicentral azimuth taken from the Wiechert seismograms were small or not.

3. Observations

Earthquakes, whose initial displacements were undoubtedly observed and the positions of whose epicenters had been accurately determined, are tabulated in Table 1, in which the true azimuth (A) of the epicenter was measured from the north in clock-wise sense and the difference (γ) between the observed and the true azimuths was taken as positive when the former was deflected in clock-wise sense from the latter. This angle of difference will be called the angle of deflection in the following pages. The positions of the epicenters were generally taken those reported in the Kisyô-yôran, but in the small local earthquakes, they were determined from the observed durations of preliminary tremors at Beppu and Aso by using Omori's formula, their depths of origon being estimated from the observed emergent angles, taking into consideration the results of observation of earthquakes which occurred in nearly the same district, and their epicenters were accurately determined from observations at various stations. The error in position of a seismic focus determined from observations of the time of occurrence and the duration of preliminary tremors at

1. These Memoirs, A. 18 (1935), pp. 255–293.

Table 1

No.	Date					at Beppu			at Aso			Origin	
						A	γ	P–S	A	γ	P–S	φ	λ
			d	h	m			m s			m s	N	E
1	1929	June	3	6	39	76°	3°	60.8	72°	– 4°	56.0	34.°3	136.°8
2			13	9	13	47	– 3	4 2.7	47	–26	3 50.0	44.4	150.2
3			13	18	27	203	–23	4 26.6	203	– 2	4 37	15	124
4		Aug.	4	1	00	323	16	15.8				34.3	130.6
5			8	22	33	281	48	13.5	318	– 8	16.5	33.4	130.4
6		Oct.	25	3	57	229	–27	20.0	236	–13	8.3	32.6	130.4
7	1930	Feb.	5	22	28	282	32	16.5	316	–12	12.7	33.5	130.3
8			7	12	34	282	40	12.8	316	–15	12.6	33.5	130.3
9			27	21	10	148	–10	16.5	116	29	17.0	32.3	132.5
10		May	1	9	58	72	– 8	1 47.5	70	– 4	1 48.4	36.4	140.8
11			24	1	38	81	– 9	1 18.0	77	– 3	1 26.8	34.2	139.6
12		June	1	2	58	68	0	1 50.8	64	–12	1 47.0	36.4	140.4
13		July	23	4	26	45	2	3 14.0	45	–27	3 17.2	44.3	149.0
14		Aug.	21	5	54	225	–30	2 23.0	225	–14	2 23.8	24.5	122.2
15		Nov.	26	4	3	72	7	1 30.1	70	– 7	1 33.7	35.1	139.0
16		Dec.	13	1	4	227	–21	9.6				32.87	130.96
17			20	23	2	39	– 1	25.4	40	–28	31.8	34.8	132.9
18			21	21	14	39	1	26.0	40	–17	32.3	34.8	132.9
19			21	23	51	227	–40	2 55.9					
20	1931	Jan.	29	11	54	192	–38	41.3	186	0	38.0	30.4	130.7
21		Feb.	13	9	41	225	–23	2 16.0	225	– 9	2 10.9	24.3	122.0
22		Mar.	9	12	49	45	– 5	2 45.5	45	–30	2 46.0	40.6	141.9
23			30	2	52	43	– 7	2 48.0	43	–25	2 52.0	42.6	144.2
24		Apr.	21	9	3	41	0	1 10.2	33	–34	1 13.5	38.5	134.2
25		June	2	11	38	64	– 9	1 3.5					
26			23	15	15	66	1	1 40.0	64	– 7	1 48.0	36.5	141.7
27			30	1	43	81	– 3	59.0				33.9	136.8
28		Sept.	22	17	36	164	–22	17.3	136	28	15.0	32.2	131.8
29		Oct.	8	7	6	56	0	9.8	50	–21	15.6	33.6	132.0
30		Nov.	2	3	52	158	–12	17.0	122	18		32.4	131.9
31			2	17	32	130	24	17.5	105	8	20.0	32.5	132.5
32			3	0	47	150	–10	17.0	118	20	17.0	32.4	132.0
33		Dec.	19	2	45	173	–31	22.1	150	21	18.2	32.0	131.6
34			21	14	47	226	–16	19.8	230	–15		32.5	130.4
35			22	22	8	226	–17	18.2	230	–14		32.5	130.4

Table 1 (Continued)

No.	Date				at Beppu			at Aso			Origin	
					A	γ	P–S	A	γ	P–S	φ	λ
			d	h m			m s			m s	N	E
36		Dec.	26	10 43	226°	-20°	19.9				32.°5	130.°4
37	1932	Jan.	3	6 53	127	23	22.0	108°	29°	24.0	32.2	132.9
38			3	12 11	143	-13	18.0	114	23	19.0	32.4	132.2
39			27	21 16	170	-21	18.0	139	25	14.8	32.3	131.6
40		Feb.	15	10 6	136	10	18.2	109	44	20.1	32.5	132.4
41			15	6 32	216	-15	33.0	211	3	27.0	30.8	130.3
42		March	17	9 50	139	13	15.8	110	30	18.0	32.5	132.2
43		May	3	8 29	180	-15	29.5	168	21	23.0	31.4	131.1
44			5	13 11	62	- 4	51.4	59	-12	58.2	35.0	135.6
45			28	11 21	185	-16	55.0	180	- 1	51.0	29.2	131.3
46			28	14 3	185	-31	54.9				29.5	130.8
47		June	8	15 14	165	-18	18.4	142	24	18.3	31.9	131.8
48			8	19 54	161	- 8	19.1	132	38	18.2	32.2	131.9
49			18	10 31	130	7	13.0	100	7		32.7	132 3
50		July	25	17 25	56	0	56.8	54	-25	1 26.6	35.6	135.6
51			27	9 30	100	- 2	1 16.5	97	3		31.9	139.0
52		Aug.	21	13 16	227	-43	2 30.3	227	- 7	2 24.0	24	122
53		Sept.	3	20 59	47	- 2	3 1.5	47	-19	3 1.6	41.0	143.1
54			29	12 42	306	35	14.6				33.7	130.7
55			30	2 48	48	- 7	4 6.2	48	-20	4 2.8	42	147
56		Oct.	24	6 28	224	-29	2 20.6	224	-10	2 23.2	24.2	122.3
57			26	2 3	33	- 3	2 59.3				46.3	145.3
58		Nov.	26	13 24	41	-16	2 25.6	41	-26	2 14.6	42.3	142.3
59	1933	Feb.	9	12 57	103	- 4	1 14.5				31.7	138.8
60		March	3	2 31	58	- 6	3 36.1	58	-11	3 30	39.1	144.7
61			12	4 33	118	3	1 48.0	114	13	1 45.2	28.9	140.9
62			12	16 38	51	- 5	12.3	50	-15	22.0	34.0	132.6
63			19	0 51	95	2	1 21.1	91	- 1	1 23.1	32.4	139.7
64			22	8 18	223	-16	6.8				32.87	131.03
65			25	21 50	227	-15	7.5				32.89	130.99
66		April	13	12 53	228	-11	6.8				32.90	131.00
67			19	15 44	225	-23	2 38.3	225	- 9	2 29.9	24.3	121.7
68		May	5	20 38	221	-12	8.5				32.89	131.07
69			5	20 54	223	-13	6.3				32.88	131.04
70			5	21 4	227	-13	7.8				32.89	130.59

Table 1 (Continued)

No.	Date					at Beppu			at Aso			Origin	
						A	γ	P–S	A	γ	P–S	φ	λ
			d	h	m			m s			m s	N	E
71	1933	May	15	10	17	224°	-14°	7.0				32.88	131.02
72			23	5	44	161	-16	18.9	134°	30°	17.8	31.9	131.8
73			24	1	36	176	-12	29.5	162	26	24.0	31.4	131.7
74			24	1	52	183	-20	33.5	172	-15	30	31.2	131.4
75		June	2	16	39				174	6	28.0	31.7	131.1
76			19	6	37	58	- 8	2 16.2	58	-11	2 20.5	38.5	142.8
77		July	10	9	22	56	- 5	2 16.2	56	-29	2 37.0	38.9	144.8
78			18	20	22	206	-42	54.9	205	- 5	51.0	28.8	129.0
79		Aug.	16	13	10	227	-19	9.3				32.89	131.00
80			25	16	54	280	14	4 15.5	280	- 4	4 11.3	34	102
81		Sept.	3	1	42	111	- 1	1 25.6	107	13	1 26.6	30.3	139.4
82			16	1	20	184	-22	59.6				29.3	130.4
83		Oct.	4	3	39	54	6	2 14.3	54	-22	1 45.0	37.2	138.8
84		Dec.	5	4	34	35	-10	2 53.3	35	-40	2 57.7	45.2	144.0
85	1934	Jan.	15	17	49	227	-22	7.2				32.95	130.97
86		Feb.	14	13	0	203	-17	3 28.0	203	- 2	3 26.2	15	124
87			24	15	24	123	13	2 50.7	120	7	2 53.0	24.5	145.0
88		Jan.	9	8	7	70	0	37.4	65	-14	44.0	34.0	133.9
89		March	30	23	54	140	15	20.2	120	35	20.0	32.3	132.1
90		April	15	19	33				76	- 5	1 37.0	34.5	140.0
91			20	1	14				103	6	1 23	31.0	139.5
92			28	11	1	289	43	12.0	327	-16	12.0	33.57	130.40
93		June	3	6	29	168	-18	21.0				31.7	131.9
64		Sept.	1	8	5	0	18	8.3	18	-18	13.6	33.8	131.4
95		Oct.	27	2	11				163	18	44.0	30.5	132.0

A: True azimuth. γ: Angle of deflection. P–S: Duration of preliminary tremors.

various stations is, in well determined case, less than 10km. when the earthquake occurs on land, and about 50km. for an earthquake in the ocean and remote from land. Taking these facts into consideration such earthquakes were omitted from the present study as their errors in observed angle of deflection, due to possible errors in determining the position of the seismic foci, were considered to be not less than 5°. Figs. 1 (a) and (b) show the azimuthal distribution of the angles of deflection of seismic rays observed at Beppu and at Aso. The near earthquakes with durations of preliminary tremors shorter

than 20 seconds are indicated by black circles and the intermediate earthquakes with tremors of 20 seconds to 2 minutes, by single circles and the distant earthquakes with tremors longer than 2 minutes, by double circles. As shown in Figs. 1, the azimuthal distributions of

Fig. 1. Azimuthal distribution of the angle of deflection of seismic rays observed.

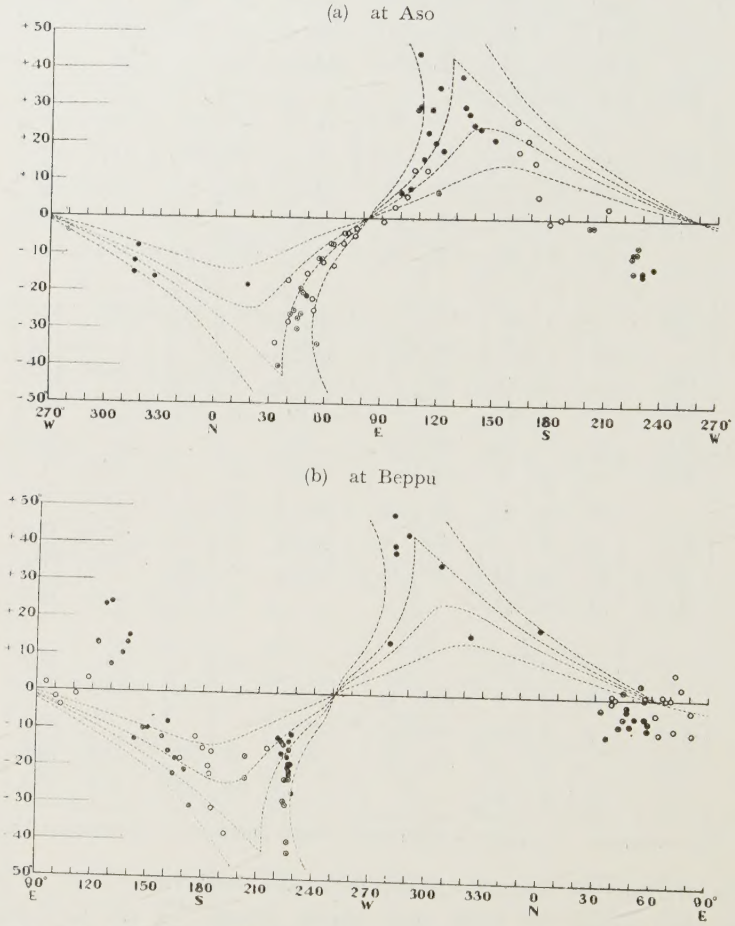

the angles of deflection observed are fairly systematic but no definite relation between the angle of deflection of seismic rays and their epicentral distances can be found, though it probably existed. At the Aso Volcanological Laboratory the seismic rays, which came from the northern side were deflected in the negative sense, the maximum angle of deflection being about 40° in the NE azimuth; and those from the southern side in the positive sense, the maximum angle of deflection

being about 40° in the SE azimuth, excluding the seismic rays from the SW direction which were deflected in the negative sense.

The azimuthal distribution of the deflection of seismic rays observed at the Beppu Geophysical Laboratory is quite similar to that observed at Aso if the epicentral azimuth for Beppu is measured from the south instead of from the north as in the case of Aso.

4. Considerations

As it was doubted that the discrepancies between the observed and the true epicentral azimuths were due to some instrumental errors, introduced from friction or from some unknown instrumental defects, the comparison between the records of earthquakes registered by the Wiechert seismographs and by the carefully adjusted micro-seismographs, Type G_A, was made at the Aso Volcanological Laboratory. All earthquakes tabulated in Table 2, only 11 in number for the reason already stated, are those which were recorded by both of the above two instruments.

Table 2

	A_w	A_g	A_g-A_w	γ
1933 July 10 9^h	27°.5	25°.3	−2.°2	−29°
1932 Sept. 30 2	28.4	32.2	3.8	−20
Sept. 30 13	90.0	90.0	0	
July 27 9	97.3	100.2	−2.9	5
May 27 1	108.2	111.8	3.6	
Sept. 27 4	112.1	112.3	0.2	
June 8 15	166.3	165.6	−0.7	24
June 8 19	170.4	170.3	−0.1	38
1933 Apr. 19 15	216.8	213.7	−3.1	− 9
1932 Aug. 21 13	220.3	218.7	−1.6	− 7
Sept. 23 23	353.4	353.0	−0.4	−31
Mean			1.7	

Where A_w is the azimuth observed by the Wiechert seismograph and A_g that observed by the G_A type micro-seismographs and γ is the angle of deflection calculated from A_w.

As the G_A type instruments are considered to be free from friction and have a high magnification as compared with those of Wiechert, the observed azimuths obtained by the former are to be considered as giving nearly correct values. The difference between the azimuths observed by the two instruments was only 1.°7 in the mean and 3.°8

even in the maximum, while the angles of deflection observed were much greater than this, being as much as ca. 30° for certain azimuths. So the cause of the anomalous deflection of seismic rays cannot be taken as due to instrumental or observational errors. The results of comparison between the records of earthquakes obtained by the Wiechert seismograph with those by the Omori portable tremor recorder made at the Beppu Geophysical Laboratory are given in Table 3.

Table 3

		A_w	A_o	$A_o - A_w$	γ
1932 Nov.	13 15^h	23°.2	31°.2	8°.0	
July	25 17	56.3	55.8	−0.5	0°
May	5 13	58.2	50.8	−7.4	− 4
Jan.	9 19	135.0	130.2	−4.8	
June	18 10	137.3	128.0	−9.3	7
1931 Dec.	19 2	142.9	144.1	1.2	−31
1932 June	8 15	147.3	146.3	−1.0	−18
Jan.	27 21	149.0	149.3	0.3	−21
March	17 9	152.2	144.3	−7.9	13
June	8 19	152.9	158.1	5.3	− 8
May	3 8	165.3	162.9	−2.4	−15
1319 Dec.	26 10	206.2	204.4	−1.8	−20
Dec.	21 14	207.3	199.3	−8.0	−19
Mean				4.5	

The azimuths recorded by the Omori portable instrument are generally more deviated from the true epicentral azimuths than those recorded by the Wiechert instrument, but the difference between the azimuths observed by the two instruments was about 4.°5 in the mean and 9.°3 in the maximum, as shown in the fourth column of Table 3, while the angles of deflection observed were much greater than this, being about 30° for certain azimuths as shown in the last column. Therefore we see once more that the cause of anomalous deviations of the observed azimuths from the true epicentral azimuths cannot be taken as due to instrumental or observational errors only, and their main causes should be sought in certain anomalies in the geological structure of the upper-crust of the two volcanic districts. In the case of distant earthquakes, the period of their initial motions is about 5 seconds or more, while that of near earthquakes is about 1 second or less, and their corresponding wave lengths are therefore to be taken as of the order of about 20km. and 4km. respectively. This

notwithstanding, the observed amounts of the lateral deflections of seismic rays are nearly the same in both cases, independently of their wave-lengths, and so the degree of anomaly in geological structure of the upper-crust sufficient to cause the described lateral deflections of seismic rays cannot be very small compared with the wave-lengths of about 20km. or more.[1] Moreover the seismic rays of such earthquakes with epicentral distances so near as ca. 40km. showed the same amount of lateral deflection as those of more distant earthquakes. Therefore the special geological structures of the upper crust sufficient to cause the lateral deflection of seismic rays must be considered as being within about 40km. of the observatories. Looking now at the topographical and geological map of the volcano Aso, the famous great caldera of nearly circular form of about 20km. in diameter has our attention. According to Prof. T. Matsumoto,[2] volcanic rocks found at places along the outer side of the caldera, such as the volcanic rocks of Tawara-yama, Kura-dake, and Ôgi-dake, etc., are older than the so-called Aso lava which covers almost the entire surface outside the somma and the volcanic rocks of the central cones rising in the great caldera, and it is quite natural to assume a discontinuous boundary of nearly circular cylindrical form of 20km. in diameter, with its axis vertical somewhere near the top of Narao-dake as shown in Fig. 2. Both the older volcanic rocks outside the boundary and the newer inside are a kind of andesite, and though their elastic constants are not determined, it is not improbable that the velocity of propagation of seismic waves in the old rocks is larger than in the newer. Assuming the ratio of the velocities of propagation of the longitudinal wave outside the boundary to that inside to be 1.2 from determinations made at other places, the angles of deflection of seismic rays for distant earthquakes were calculated for four cases, in which the angles of incidence in the plane perpendicular to the surface of the earth are 0°, 37°, 45° and 51°, while their azimuthal distribution is as shown by the dotted curves in Fig. 1 (a). All the observed angles of deflection seem to be qualitatively in rough harmony with the calculated curves except for the SW azimuth, as shown in Fig. 1 (a). Of course the discontinuous boundary may not be of simple circular cylindrical form, and moreover the observational errors for the emergent angles are much greater than those for the azimuths, so we must be

1. M. Hasegawa: Zeit. f. Geophy. 6 (1930). K. Sezawa: Bull. Eqke. Res. Inst. 3 (1927).
2. T. Matsumoto: "New study on the great volcano Aso."

Fig. 2. Map of the Volcano Aso.

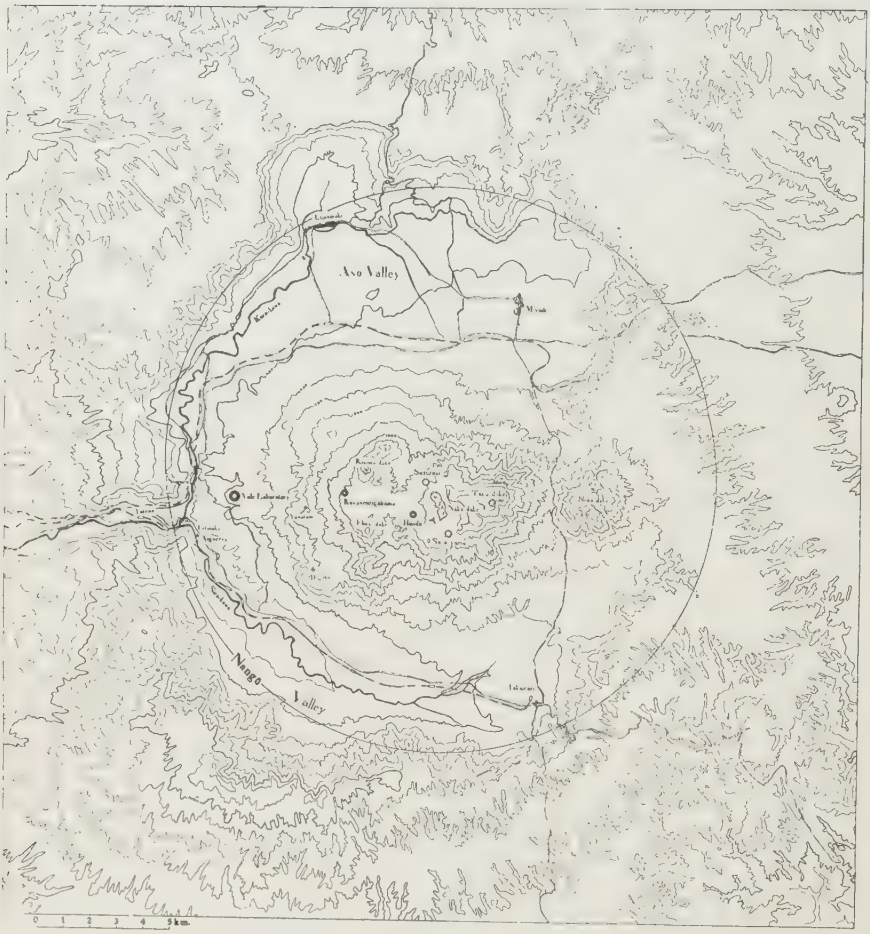

content with a qualitative comparison of observations and rough calculations, waiting for further accumulation of observational data at selected stations for the special purpose. The discrepancy between the observed and the calculated angle of deflection for the SW azimuth is probably due to the great Tateno barranco which belongs to the great rupture line running in the E-W direction. The azimuthal distribution of the angles of deflection observed at the Beppu Geophysical Laboratory is quite similar in character to that observed at Aso, and so it is reasonable to assume the existence of a discontinuous boundary at Beppu similar to that at Aso. There is no topographical boundary at Beppu corresponding to the great caldera at Aso, but

there is the active volcano Turumi-dake at a distance of 5km. west of the laboratory, corresponding to the active volcano Naka-dake at a distance of 7.5km. east from the Aso Volcanological Laboratory and, corresponding to the Five Central Cones of Aso, there are Turumi-dake, Yuhu-dake and Iwoo-dake at Beppu. According to the late M. Suzuki, formerly Assistant Professor of our Geophysical Laboratory, the volcanic rocks of Turumi-dake, Yuhu-dake and Iwoo-dake were found to be younger than those in their environment. Therefore it is not unreasonable to assume a cylindrical boundary as shown in Fig. 3.

Fig. 3

Assuming the same velocity ratio of the outside to the inside of the boundary as in the case of the Volcano Aso, the angles of deflection calculated for the same four different cases of incident angles in the vertical plane as at Aso for distant earthquakes are given by the dotted curves in Fig. 1 (b), the distribution of observed angles of deflection being fairly satisfactorily explained on the whole. But the observed angles of deflection of seismic rays coming from the azimuths E30°S–E50°S do not show any correspondence with the calculated values. This discrepancy is more probably due to the great fault running from Horita to Hotoke-zaki, and then dipping deep into the sea at the point where Uryû-sima sank to a considerable depth in the great earthquake of the Keityô-era (1596). The angles of deflection of seismic rays of earthquakes occurring in the Aso volcanic district and in the island of Formosa, and the ratios of the vertical to the horizontal components of their initial motions as observed at the Beppu Geophysical Laboratory, are as given in Table 4 and Fig. 4, showing that the angles of deflection are much greater for earthquakes of greater emergent angles, which is, qualitatively, in harmony with the calculation.

Table 4

Aso earthquakes

No.	Date	A	γ	V/H
68	1933 May 5 20^h	221°	−12°	0.58
69	May 5 20	223	−13	0.80
67	Mar. 25 21	227	−15	0.85
70	May 5 21	227	−13	0.86
71	May 15 10	224	−14	1.12
63	Mar. 22 8	223	−16	1.17
85	1934 Jan. 29 10	227	−22	1.50
79	1933 Aug. 16 13	227	−19	1.75
16	1930 Dec. 13 1	227	−21	2.38

Formosa earthquakes

No.	Date	A	γ	V/H
66	1933 Apr. 19 15^h	225°	−23°	0.41
57	1932 Oct. 24 6	224	−29	0.55
14	1930 Aug. 21 5	225	−30	0.60
21	1931 Feb. 13 9	225	−23	0.85
19	1930 Dec. 21 23	227	−40	1.22
52	1932 Aug. 21 13	227	−43	2.80

If a discontinuous boundary of the upper crust really exists, as assumed for Beppu and Aso, the amplitude of seismic waves observed should be greatly dependent, in consequence, on their angles of incidence on the discontinuous boundary, owing to their refractions and reflections there-at, and generally speaking, the greater the

Fig. 4.

● : the Aso earthquakes, ○ : the Formosa earthquakes

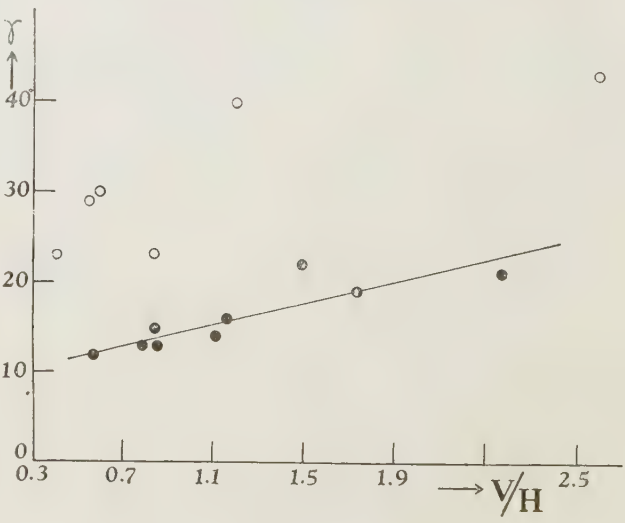

angle of deflection of the seismic rays the more should the amplitude of the seismic waves recorded at the laboratory be reduced. This expectation is not contrary to the observed facts and the following Hukuoka earthquake of April 28, 1934 is one of the best examples. The epicentral distances of the mentioned earthquake from Beppu and Aso were approximately the same, but the amplitudes of the earthquake waves recorded at Beppu were exceedingly small, being only one-seventh, or less, of those observed at Aso in every phase of the waves, as will be seen from Plate I. The above fact cannot be explained from any assumption on the mechanism of occurrence of the earthquake, and the only explanation is the above assumed refraction effect at a discontinuous boundary. The angle of deflection of the initial motion observed at Beppu was 43°, which corresponded to that of the seismic ray incident on the assumed discontinuous surface at nearly the grazing angle, and almost all the energy of the earthquake waves is reflected in this case, only a small fraction of energy being refracted into to be observed at the Laboratory. On the contrary the observed angle of deflection of the initial motion of the earthquake was 16° at the Aso Volcanological Laboratory, which corresponded to that of the seismic ray with the incident angle on the discontinuous surface at about 50°, and nearly all the energy of the incident waves was refracted into to be observed. One of the other interesting phenomena due to such a discontinuous boundary is the accumulation of energy of the seismic wave within the boundary owing to its focussing effect, but consideration of this phenomenon will be postponed to the next occasion. The scattering effect of seismic rays due to the reservoir of molten lava under the active vent is also to be noticed as giving an azimuthal distribution of the angle of deflection of seismic rays for certain wave-lengths similar to that above described, and this makes an interesting study on the internal condition of the reservoir, but the amount due to this cause is not so great as those mentioned above, for the dimensions of the obstacle, the reservoir of molten lava, are not large enough as estimated from the observations of volcanic micro-tremors and eruption-earthquakes.

While waiting for further accumulation of observational data, the present author concludes this preliminary report by referring to a note about the related problem due to Prof. Saem. Nakamura. He reports,[1] that according to observations made at the western foot of

1. Saem. Nakamura: "Disin" 1 (1929).

Tokati-dake, Hokkaidô, seismic rays perpendicular or parallel to the Nuputatesike-range were not deflected, but those which crossed the the range from SE to NW were deflected greatly to the north, and he sought the explanation of this phenomenon in the refraction of seismic rays at a discontinuous boundary parallel to the range. He also states that a somewhat similar anomalous deflection of seismic rays was observed at Numadu, but the data reported are not sufficient for a detailed study of the structure of the upper crust in this area.

Plate I

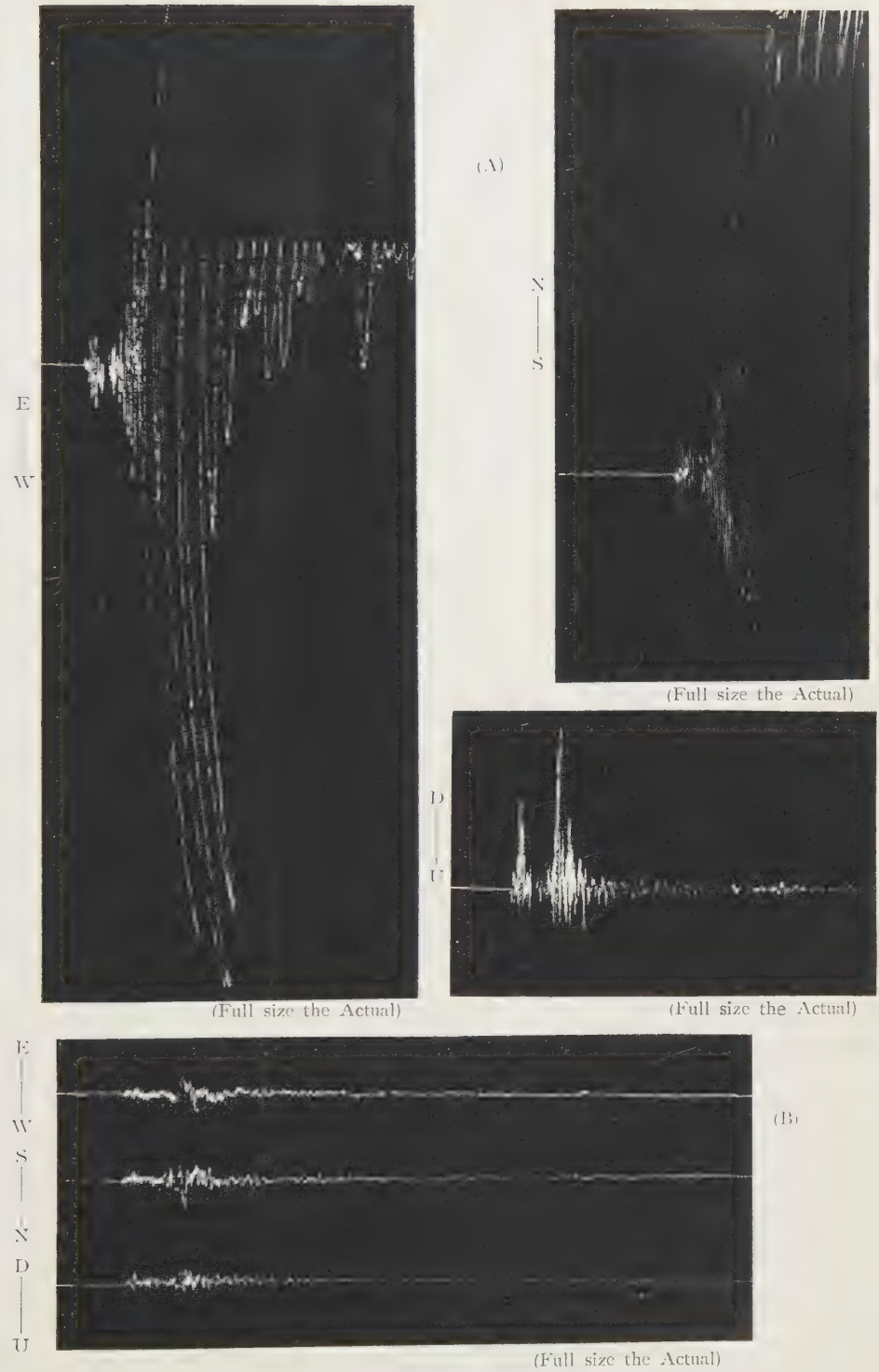

Fig. 5. Seismograms (full size of the actual records) of the earthquake of April 28, 1934 obtained at Aso (A) and Beppu (B). (1 min. = 30 mm.)

		T_0 sec.	ν	I
Instrumental constants:	Aso: Horizontal comp.	10.0	4 : 1	200
	Vertical comp.	4.6	4 : 1	150
	Beppu: Horizontal comp.	12.0	4 : 1	200
	Vertical comp.	4.6	4 : 1	150

A View of the Structure of the "Muroto Typhoon"

By Tadao Namekawa and Shiichi Aoki

(Received November 22, 1935)

Abstract

When the Muroto Typhoon, after traversing Shikoku, passed the Kinki District, its power was immeasurably great. In the records of the time, taken at each meteorological observatory, several peculiarities are found. In order to explain these peculiarities, the authors assumed that the typhoon was not single, as might appear, but was composed of two cyclonic systems of different nature. What the authors call the "Main Typhoon" is the typhoon whose track can be traced for more than ten days, from the time it made its appearance till after it had passed over Japan, and whose pressure at the centre remained at about 730 mm. Hg., while it was passing over Japan. On the other hand, what the authors call the "Secondary Typhoon" is considered to have been a shallow disturbance restricted to the lower layer, its circulation system belonging to the tornado-type. Although the development and dissipation of this disturbance is very rapid, its scale is vastly greater than that of an ordinary tornado. Its original state is not clear, as it was formed over the sea, but it had its maximum intensity in the neighbourhood of Muroto Point, and weakened down to the level of an ordinary secondary cyclone in the neighbourhood of the Noto Peninsula, meanwhile appearing on weather charts like the Main Typhoon. In the following paper, the authors have tried to elaborate the above view.

1. On the morning of Sept. 21, 1934, the western part of Japan, viz., *Shikoku* and *Kinki*, was attacked by a severe typhoon, and not a little damaged. As the typhoon recorded the lowest pressure, 684.0 mm. Hg. (reduced to the sea-level) at Muroto Point, the Japanese meteorologists decided to call it the "Muroto Typhoon." From the meteorological point of view, and also in respect of the amount of damage it caused, it was unprecedented in history, and numerous reports of investigations have already been published. A detailed examination of the typhoon is made in the Report of the "Muroto Typhoon"[1] published by the Japan Central Meteorological Observatory, and all available data are given without a single omission. When the authors set about to make researches into this typhoon, they noticed that it had certain peculiarities, and in order to explain them, they came to the conclusion that this typhoon consisted of two cyclonic systems of different nature. This paper was drawn up with the purpose of substantiating this view, and those who are interested in general investigations or those who wish to pass judgment on the authors views, are requested to refer to the reports just mentioned.

1. Report of the "Muroto Typhoon". Central Met. Obs. Japan. (1935).

2. First of all, attention must be drawn to the isochronous curves showing the time when the minimum pressure was recorded at each meteorological observatory, as the typhoon passed along. Generally speaking, it is the nature of these curves that they form lines perpendicular to the travelling direction of the cyclone, and passing its centre. But from 5h to 10h, that is, while the typhoon was at its height, the isochronous curves show a remarkable bend, lagging about an hour behind near the centre, as compared with parts further away. This bend disappears after 11h. If the minimum pressure be identified with the centre of the typhoon, as in the Preliminary Report of the "Muroto

Fig. 1

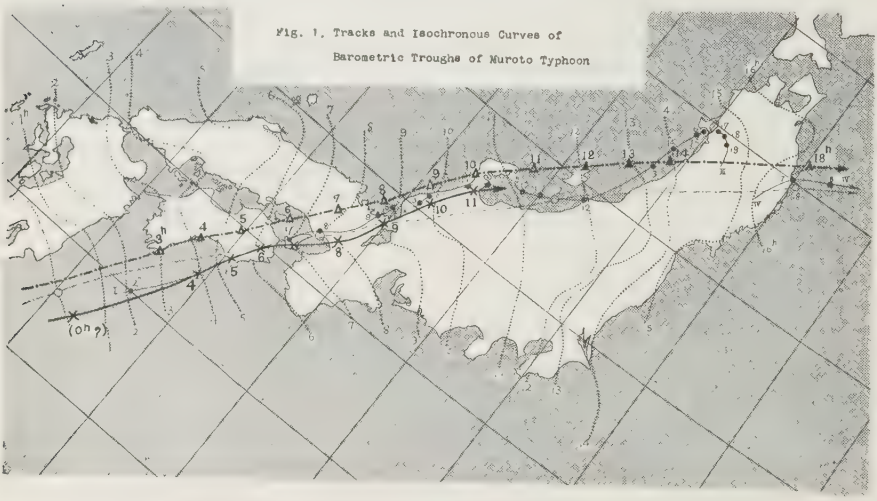

Fig. 2. Weather Chart.

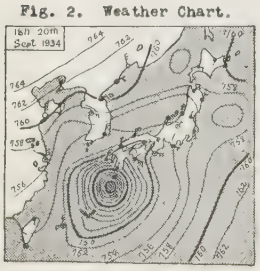

Fig. 5. Weather Chart.

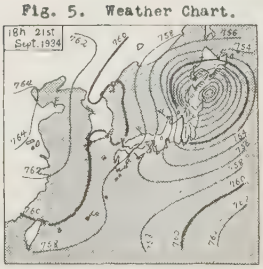

Typhoon" published by the Central Meteorological Observatory,[1] the mean velocity of the typhoon, from 9h to 12h, is 117km/hour, which differs considerably from the velocity of 60–80 km/hour before and after that period. In the Report just mentioned, this increase of apparent velocity is considered as having

1. Preliminary Report of the "Muroto Typhoon." Central Met. Obs. (1934) p. 5.

Fig. 3–5 7–8

Fig. 3. Weather Chart, 6h. 21st. Sept. 1934.

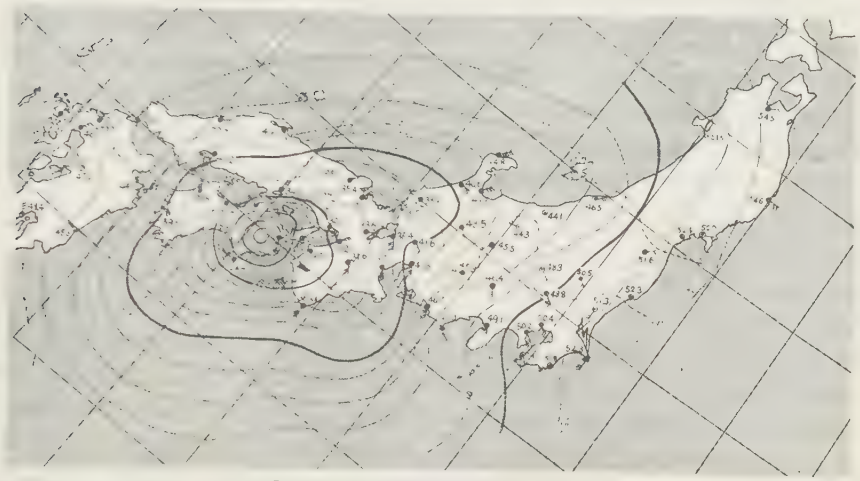

Fig. 4. Weather Chart, 9h. 21st. Sept. 1934.

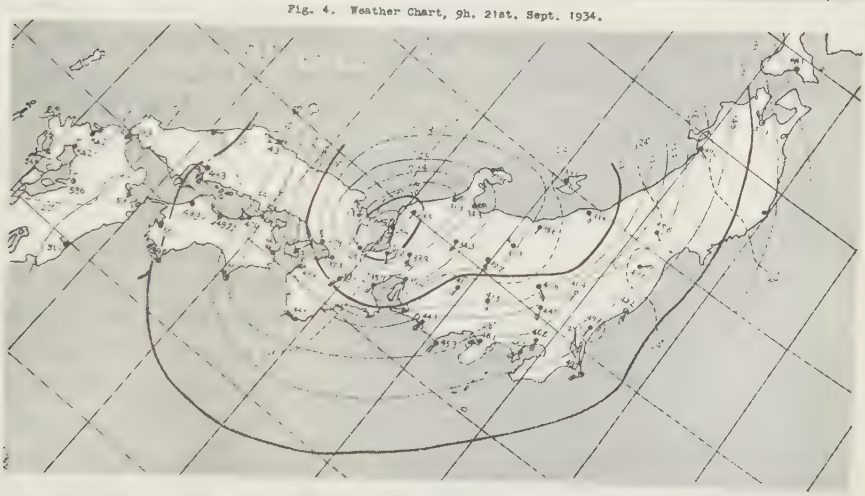

Fig. 7. Calculated Isobars, at 6h. 21st.

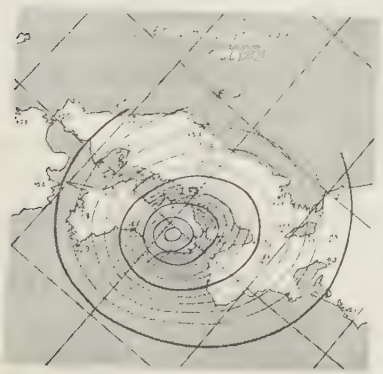

Fig. 8. Calculated Isobars, at 9h. 21st.

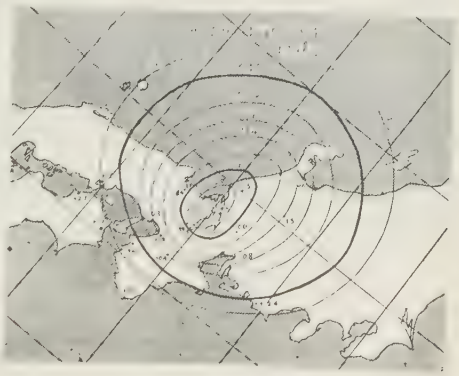

been due to the precedence of the head of the typhoon. The corresponding track of the typhoon is shown by —○—○—○→ in Fig 1. Dr. Y. Horiguchi,[1] after carefully examining the available data, concluded that a succession of the typhoon occurred in the Bay of Wakasa. The track corresponding to his investigation is shown as —●—●—●→ in Fig. 1. After having examined these views, the authors came to their own conclusion, which is submitted to the readers' judgment here below.

3. In the next place, in the four weather charts shown in Figs. 2–5, no remarkable dissipation is found in the isobars greater than 740 mm. Hg., whereas in the charts for 6h and 9h, a remarkable dissipation is found near the minimum pressure. In fact, at 6h the pressure at the centre is presumed to be about 700 mm. Hg., and at 9h, 720 mm. Hg. Although it stands to reason that, when a cyclone passes over land it loses in intensity, such a partial dissipation appearing only in the central portion, as found in this case, presents a special problem.

4. Now, considering a typhoon to be a case of revolving fluid, the wind records at various localities were examined. The most noteworthy point in the Kyôto record, given in Fig. 6, is a peculiar feature between 8h and 10h. This cannot be satisfactorily explained by supposing that it was caused by the passing of a single revolving fluid. That there is a change in the record from 8h 20m SE 30–40 m/s to 9h 40m W 25–30 m/s leads us to the assumption that a powerful whirlwind superposed its own wind system on another wind system. Now we suppose that the time interval between the front (the maximum wind zone)

Fig. 6

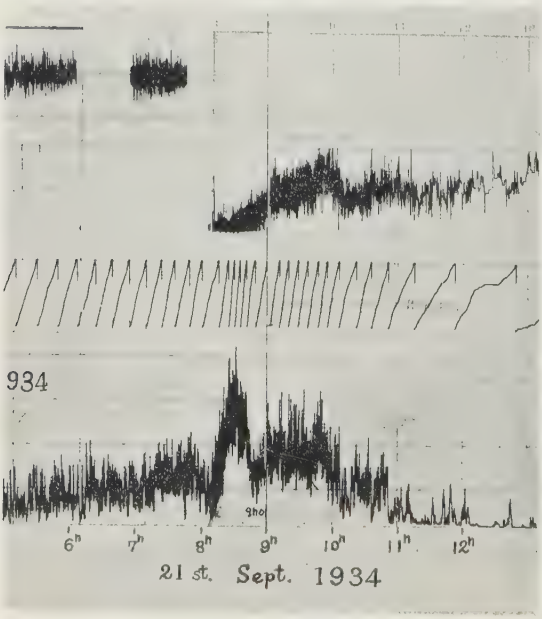

Wind-Record at Kyôto.
(Met. Inst. Imp. Univ. of Kyôto)

1. Report of the "Muroto Typhoon" pp. 42–80.

and that of the rear was 80 min., and that the velocity of translation of this whirlwind was 80 km/hour; we then estimate that the diameter of the whirlwind system was about 100 km. In the wind records at *Muroto* and *Tokushima*, similar traces of the whirlwind can be found. The dimension of this whirlwind system is too small for it to be supposed that it covered the whole typhoon. Therefore, it is reasonable to consider that it is an entirely different system accompanying the typhoon.

5. Thus the authors assume that, besides the typhoon in question, another whirlwind system existed. As this system was exceedingly powerful from 4h to 11h, a remarkable lowering of pressure occurred near its centre, which, accordingly, looked as if it were the centre of the typhoon on the weather charts. In other words, when one tries to identify the centre of the typhoon on the weather charts, without due consideration, one actually finds the centre of the whirlwind or "Secondary Typhoon" as we call it; its position is shown by —×—×—×→ in Fig. 1. The Secondary Typhoon rapidly dissipated and, after 11h, looked like an ordinary secondary cyclone on the weather map. As this stage, the minimum of pressure coincides with the centre of the typhoon proper, not with the centre of the Secondary Typhoon as previously. Therefore, the position of the centre of minimum pressure after 11h is shown by —▲—▲—▲→ in Fig. 1, thus identifying it with the centre of the Main Typhoon. The track of the Main Typhoon, while under the influence of the Secondary Typhoon, cannot be obtained directly from the weather map. Its path, shown by —△—△—△→ in Fig. 1, is inferred from the known features before and after the epoch—namely, by inferring its actually unknown position from its context, and interpolating its path as a comparatively smooth curve. Its position at each hour was obtained by dividing the curve uniformly, but that each position roughly corresponds to the isochronous curve of minimum pressure endorses our assumption.

6. If the Muroto Typhoon is supposed to have had the structure above described, its peculiarities become clear. The Main Typhoon passed over without any remarkable change of intensity, whereas the Secondary Typhoon rapidly diminished in intensity as it traversed the land. This fact is physically considered below. Concerning the height of tropical cyclones, there are two conflicting theories—the one, held by Hann[1] and E. W. Newnham,[2] is that they are shallow disturbances,

---

1. Lehrbuch der Meteorologie, (4th edition 1926) p. 620. 2. Geophys. Memoir No. 19, Met. Office, London (1922) p. 232.

and the other, held by Sir. W. N. Shaw and B. Haurwitz,[1] is that they are not. What the authors call the Main Typhoon is a long-lived system with a considerable persistency and cannot be treated as a shallow disturbance. At least, the whole tropospheric air must be considered as being in rotation. This Main Typhoon is a well-developed cyclone, similar to what Sir. W. N. Shaw calls a "Circular Depression".[2] On the other hand, the Secondary Typhoon is the shallow disturbance of a short-lived system, which is endorsed by its rapid dissipation. Moreover, when the severe typhoon had passed, the damage was even smaller on *Mt. Rokko* and *Mt. Hiei* than on the low-lying plains. There is no information about the Secondary Typhoon at the time of its first appearance, though it is surmised that it developed off the southern coast of *Shikoku*. It must have been a short-lived cyclonic system resembling a whirlwind or a tornado in its development and dissipation, but on a much larger scale than a tornado, and it was, in this respect, rather like a newly-formed cyclone. It would be rash to presume that it was a phenomenon such as occurs, according to Sir. W. N. Shaw's account, when the lower part of a typhoon is cut off while passing over a mountain range; or that it was an instance of Dr. Kobayashi's theory.[3] The peculiar features of the Main Typhoon, while traversing the *Ou* District from 14h to 18h, when it reached the Pacific Ocean, can be explained by the foregoing theory, but in the case of what the authors call the Secondary Typhoon, things are rather different. Perhaps it suddenly appeared under conditions favourable for the creation of whirlwinds or tornadoes. It must also be noticed that the place where the Secondary Typhoon appeared is the place where a secondary cyclone often appears when a cyclone passes over the Japan Sea. Moreover, the discontinuous line accompanying the typhoon may have played some part in producing it. The authors have not yet reached any definite conclusion about these features, nor about the source from which the Secondary Typhoon derived its energy.

7. Here follow semi-quantitative considerations which may very possibly lead to the verification of the authors' view. This is a very difficult problem. But the authors' purpose is not to obtain an accurate expression of the field of motion and pressure of the typhoon, but to show that the deductions from their theory—that this typhoon was composed

---

1. Monthly Weather Review **63** 2 45. (Feb. 1935). 2. Manual of Met. Vol. IV p. 242. 3. Q. J. R. Met. Soc. **48** 169 (1922).

of two cyclonic systems—coincides to some extent with the actual field of motion and pressure of the typhoon. So, the authors attempted to carry out the superposition Sir W. N. Shaw's model of "Circular Depression" and Bigelow's[1] model of "Funnel Shaped Vortex", neglecting the original field and the effect of friction. But the process was too laborious, and the attempt was given up. Since, however much they might try, accuracy was not to be hoped for, they were obliged to start from the simplest possible expression. For this purpose, they decided to apply V. Bjerknes' model of the continuous vortex of the third order[2] to both the Main and the Secondary Typhoons. So, assuming

$$u = u_0 \frac{2 - \frac{y}{b}}{1 + \left(\frac{y}{b}\right)^2}$$

and also assuming that the principle of superposition is valid in the field of motion and pressure where, integrating $\frac{1}{\rho} \cdot \frac{dP}{dy} = \frac{u^2}{y}$

$$P = P_c + \frac{\zeta \left(\frac{y}{b}\right)^2}{1 + \left(\frac{y}{b}\right)^2} \qquad (2\rho u_0^2 = \zeta)$$

in our own case, the field of pressure can be shown by

$$P = P_0 + \zeta' \frac{\left(\frac{y'}{b'}\right)^2}{1 + \left(\frac{y'}{b'}\right)^2} + \zeta \frac{\left(\frac{y}{b}\right)^2}{1 + \left(\frac{y}{b}\right)^2} \cdot$$

(pressure at artificial center) (pressure change due to Main Typhoon) (pressure change due to Secondary Typhoon)

Of course, this equation is framed with reference to the dynamic principle, though not rigorously deduced. There are omissions, which are not enumerated, in various and, strictly speaking, some contradictions too. But, roughly speaking, it may safely be presumed that, from a qualitative point of view, the second term shows the pressure distribution depending on the Main Typhoon, and the third term the pressure distribution depending on the Secondary Typhoon, and that the principle of superposition applies to the field of motion and pressure.

8. Adopting the positions, already mentioned, of both the typhoons at each hour, and making use of the values of the observed pressure

1. Atmospheric Circulation and Radiation p. 196. 2. Geofy. publ. **2**. No. 4. (1921).

at that hour, we calculated P_o, ζ', and ζ by the method of least squares. We chose 50 km as the radius of the Secondary Typhoon. And that of the Main Typhoon not being accurately known, we assumed $b' =$ 200km, which may be considered reasonable from various points of view. In Table I are shown P_o, ζ' and ζ, calculated in the way above described with respect to 6h, 7h, 8h, and 9h. P_∞ in the table is the pressure value, where there is no influence from these two vortices, and shows the mean pressure of the original field. In this table, it is to be noted that P_∞ is almost constant at 749 mm. Hg., and ζ', representing the intensity of the Main Typhoon, is likewise almost constant at 17–18 mm. Hg.

Table I

time	$P_o$mm.	ζ mm.	ζ'mm.	P_∞
6h	695.0	37.8	17.1	749.9
7h	706.3	24.6	17.5	748.4
8h	715.5	15.1	18.1	748.7
9h	719.4	12.8	17.1	749.3

On the other hand, ζ and P_o diminish remarkably with the elapse of time. This points to the fact that, although the intensity of the Main Typhoon is nearly invariable, that of the Secondary Typhoon declines remarkably as time passes, and that the pressure rise at the centre depends on the Secondary Typhoon.

9. The values of pressure at each station being calculated from the proper values just mentioned by means of the above hypothetical equation, isobars are drawn in Fig. 7, and 8, which are, therefore, calculated weather maps at 6h and 9h. The figures attached to each station show the difference between the calculated and the observed values of pressure. These differences are conjoined errors resulting from insufficient assumptions and the neglect of the original field and local peculiarities. But

Fig. 9

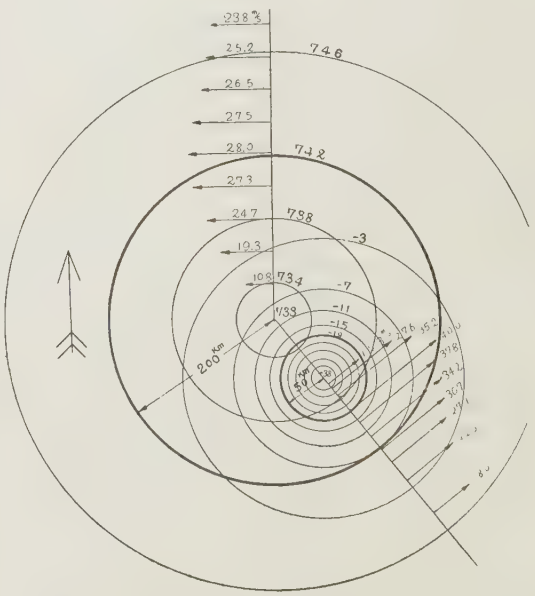

Superposition of Field of Pressure and Wind:
Calculated for the State of 6h. 21st.

the errors are unexpectedly small, and the system of calculated isobars coincides well with the characteristics of the actual isobars. Even if superposition occurs in the field of motion, the authors cannot be regard it as an effect of friction. Radial converging currents being left out of consideration, it is impossible to make a quantitative discussion. But the main feature at least can be understood from this consideration, rough though it is. As a help to this consideration, Fig. 9. has been drawn up, showing the state of things at 6h. From this figure, the reason becomes plain why a hurricane was recorded at the observatories of *Muroto*, *Tokushima*, *Ôsaka*, *Kyôto*, etc., which are situated on the right side of the two cyclones; and it also becomes clear why the wind was comparatively weak at Kôbe, which lay between the two whirlwind systems. Fig. 10 shows the meteorological elements at *Kôbe*. The kick in the barogram at about 7h and the irregular gyration of wind direction, among other things, are necessary in the authors' consideration, apart from minor differences. This trend of thought naturally brings the question of the "Typhoon Eye" to the fore. In fact, most of the stations, where the Typhoon Eye was observed in this case, are situated between the two cyclonic systems. One of the authors (T. N.) remembers that in the case of a severe typhoon which crossed Lake Biwa on Sept. 26, 1921, the calm zone was experienced not in the centre, but in its rear. If all severe typhoons are accompanied by secondary typhoons, as the typhoon in question was, it is reasonable to persue discussion of the calm zone as the authors are now doing. Moreover, when the Muroto Typhoon is analyzed, the pressure at the centre of the Main Typhoon proves to be 730 mm. Hg.

Fig. 10

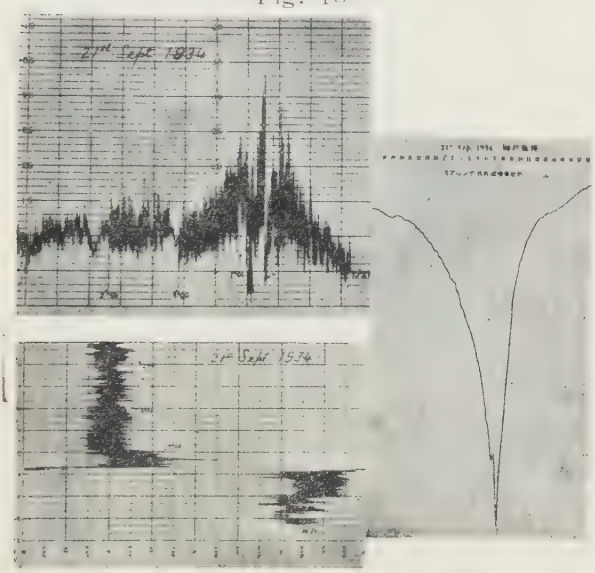

Records of Wind and Pressure at Kôbe.
(taken from Report of Muroto Typhoon.)

A suspicion arises that all well-developed typhoons have, in their normal state, this degree of pressure at the centre. In fact, typhoons of this depth seem usually to appear in our locality. And it seems reasonable to believe that, when they are especially deep, they generally have secondary typhoons appended to them, as the Muroto Typhoon had. But the authors' view of the structure of severe typhoons and the mechanism of the Typhoon Eye are very speculative at present. One of them (S.A.) is at present making investigations into recorded cases.

10. As the intensity of the Main Typhoon was nearly constant, we assumed $\zeta' = 17.5$ mm. Hg. ($u' = 30.2$ m/sec). Thence are calculated ζ, u and P_o, representing the intensity of the Secondary Typhoon from 5h to 10h. These values are shown in Fig. 11. From these values, we see that the intensity apparently diminished, after 6h, in logarithmic form, as will do all other natural phenomena. No accurate information is known concerning the typhoon for about 5h and previously, because its centre was then over the sea, and the southern coast of *Shikoku* alone was under its effect. The meteorological elements in Fig. 12. are very important. As Dr. Y. Horiguchi has noticed, the minimum of pressure is 684.0 mm. Hg. at 5h 10 m., and the wind is westerly, which is to be identified with the rear wind in the case of a cyclone. From this and from the fact that there is a remarkable fluctuation of pressure in the trough of the typhoon, he asserts the existence of a small secondary cyclone. Although, when the intensity of a cyclone is nearly uniform, the centre of the cyclone on the weather chart and the trough of the barogram ought to coincide, there may indeed be some difference between the two, while the cyclone is developing or filling. In fact, at the observatories of *Kyôto* and elsewhere, where it was recorded

Fig. 11

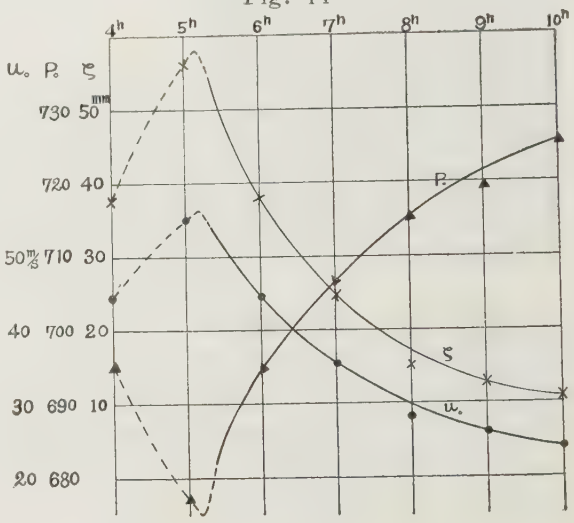

Intensities of the Secondary Typhoon.

Fig. 12

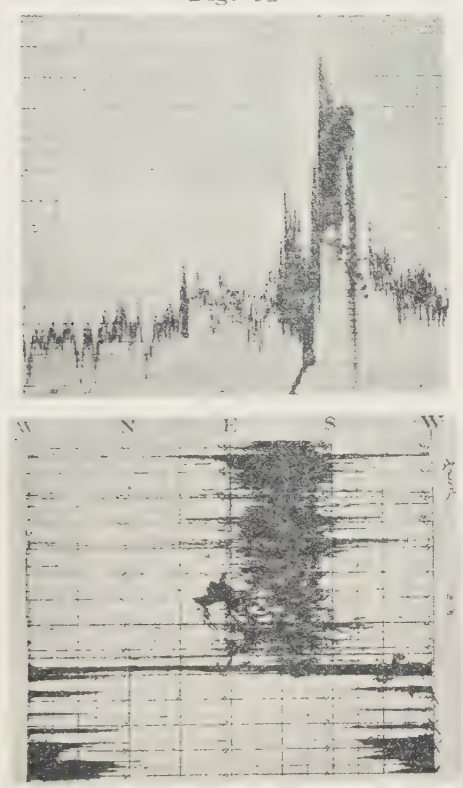

Records of Wind and Pressure at Muroto.
(taken from Report of Muroto Typhoon.)

in the filling stage, the trough of the barometric trace seems to have occurred in front of the typhoon, and that very close to the centre. On these grounds, recognizing that the barographic trough at *Muroto* lies on the rear part of the cyclone on the weather chart at 5h, the Secondary Typhoon is to be considered in its developing stage at 5h. On the other hand, in the record of the Dines Anemograph at *Muroto* the passage of the Secondary Typhoon is clearly traced, a remarkable fluctuation of wind velocity being noticed for the space of one hour. But the westerly wind in the rear is much stronger than the South-easterly wind in front, a phenomenon not observed at *Kyôto* or *Tokushima*. This contradiction is explained by the fact that at *Muroto* the circulation velocity was greater when the front maximum wind zone arrived than when the rear zone arrived. From these two facts, it seems possible to infer that the Secondary Typhoon had its maximum intensity, a little after 5h. And from the velocity of the front maximum wind at *Muroto* (wind velocity at 4h) and the pressure

values at *Muroto* and *Kôchi*, it is supposed that the Secondary Typhoon had much the same intensity at 4h as at 6h. But, as these values are less dependable than those after 6h, they are shown by dotted lines in Fig. 11.

11. The fluctuations near the barometric trough at *Muroto* are an interesting phenomenon. It may be accounted for by the influence of the direct action of the wind, the barometric oscillation, or local cyclone, etc. But these factors exist not only near the centre, but also elsewhere. It is doubtful whether they actually appeared distinctly as they chanced to be near the centre which is a stationary point in the barometric curve. In fact, it is beyond doubt that, in the case of a severe typhoon like this, numerous whirls and small secondary cyclones occur on account of orographical conditions. But the authors believe that these exercise no great influence in the case of such a vast structure as the Muroto Typhoon. It remains to be mentioned here, however, that the amplitude of the kick in the barographic curve at *Muroto* is so great that much remains over for further inquiry.

12. There is little information about the Secondary Typhoon before 6h, but there are points which seem to suggest that it made its appearance at about 0 h. on the 21st. The Japan current (Kuroshio, the warm ocean current) has perhaps some relation to its appearance. But it is impossible to ascertain under what conditions it appeared. Only, it is an undeniable fact that we have experienced instances where typhoons developed rapidly on the ocean. Further studies are required on this point.

13. Lastly, a word on the chance which led the authors to make this investigation. Through the action of the Muroto Typhoon, a remarkable bore occurred in the Bay of *Ôsaka*, which caused damage and calamities. As to the cause of the bore, one of the authors (T. N.) has expressed the view, in his discussion of seiches in the Bay of *Ôsaki*, that a bore does not occur under the influence of the typhoon itself, and that, when, a large seiche occurs on account of a microbarographic depression, its velocity coinciding with that of the long waves, the seiche swells immensely.[1] In the case of the Muroto Typhoon, the condition, $V/C \fallingdotseq -1$ was satisfied, but no microbarographic depression was recorded. And so, we came to suspect that a very intense depression of small scale existed which looked like the Main Typhoon. That is what started the authors on the above investigation.

1. These Memoirs XVIII. No. 6 (1935).

14. If all disastrous typhoons have the structure, we believe they have, the Japanese meteorologists, whose duty it is to give warning against storms, might institute a thorough investigation of the authors' view. For most of the damage is considered by us as due, not to the Main Typhoon, but to the Secondary Typhoon.

15. In conclusion, the authors wish to express their indebtedness and their thanks to the Directors of the various meteorological observatories in Japan that sent the available data of the Muroto Typhoon to the Kyôto institute: to the Director of the Central Meteorological Observatory for permission to reproduce Figs. 10 and 12, from the "Report of Muroto Typhoon": to Prof. M. Sono, Director of the College of Science of Kyoto Imperial University, and to Prof. T. Shida, Charge of the Geophysical Institute of Kyoto, both of whom gave many facilities to them; and to Dr. T. Nomitsu, Professor of Oceanography of the Geophysical Institute who gave them encouragement and criticism.

Über die Legendresche Reihe $\sum(n+1)^k P_n(x)$

Von **Yoshikatsu Watanabe**

(Eingegangen am 16, Dezember 1935)

In der vorliegenden Note[1] soll die C-Summierbarkeit der Legendreschen Reihe

$$(1) \qquad \sum_{n=0}^{\infty}(n+1)^k P_n(x) \qquad \text{für} \quad k \gtreqless 0$$

mit Hilfe ihrer erzeugenden Funktion betrachtet werden. Bei der Gelegenheit wird ein elementarer Beweis der sog. Darbouxschen Methode, welche bei der Berechnung der C-Summe so vielfache Anwendung findet, angegeben.

1. Bekanntlich sind die Legendreschen Polynome $P_n(x)$ durch

$$f(z,x)\equiv f_0(z,x)=1/\sqrt{1-2xz+z^2}=\sum P_n(x)z^n \qquad (x=\cos\theta)$$

definiert. Wird nun darauf die Höldersche Operation negativer Ordnung[2]

$$H^{-p}\equiv\left(\frac{d}{dz}\cdot z\right)^p, \qquad \text{wo } p \text{ positiv-ganz ist,}$$

ausgeführt, so ergibt sich

$$(2) \qquad \begin{aligned} f_p(z,x)\equiv H^{-p}f(z,x)&=\sum(n+1)^p P_n(x)z^n \\ &=\Phi_p(z,x)/(1-2xz+z^2)^{p+\frac{1}{2}}, \end{aligned}$$

wobei Φ_p ein Polynom von z sowie x ist; also ist

$$\Phi_0(z,x)=1,\ \Phi_1(z,x)=1-xz,\ \Phi_2(z,x)=1-xz-(2-x^2)z^2+xz^3,$$
$$\Phi_3(z,x)=1+xz-(10-2x^2)z^2+(9x-x^3)z^3+(4-5x^2)z^4-xz^5, \qquad \text{usw.}$$

Im allgemeinen gilt

$$\begin{aligned} \Phi_{p+1}(z,x)=&\{\Phi_p(z,x)+z\Phi_p'(z,x)\}(1-2xz+z^2) \\ &+(2p+1)(x-z)z\Phi_p(z,x), \end{aligned}$$

und daraus können durch vollständige Induktion folgende Beziehungen

$$(3) \qquad \begin{cases} \Phi_p(e^{\pm i0},x)\neq 0 & \text{für} \quad 0<\theta<\pi\ (-1<x=\cos\theta<1), \\ \Phi_p(z,-1)=(1+z)^p\chi_p(z) & \text{und} \quad \Phi_p(z,1)=(1-z)^p\bar{\chi}_p(z) \end{cases}$$

---

1. Ich danke den Herren Prof. Wada und Matsumoto für die sorgfältige Durchsicht meines Manuskripts und ihre gütigen Anregungen, ferner Herrn Prof. Matsumoto für seine freundliche Unterstützung, unter deren Einfluss diese Arbeit unternommen wurde und mit deren Hilfe auch einige Schwächen im Beweisgang meiner früheren Note (Über die Legendresche Reihe $\Sigma(2n+1)^k P_n(x)$ usw. I. u. II., Physico-Math. Society of Japan, Vol. **17** (1935), S. 289-) beseitigt werden konnten. 2. Y. Watanabe, Über die Äquivalenz der Cesàroschen und Hölderschen Mittel usw., Japanese Journal of Math., Vol. **9** (1932), S. 67ff.

bewiesen werden, wobei $\chi_p(z)$ und $\bar{\chi}_p(z)$ zwei Polynome des $(p-1)$-ten Grades mit nicht-verschwindenden $\chi_p(-1)$, $\bar{\chi}_p(1)$ sind.

2. Für positiv-gebrochenes $k=p-\alpha$, wo p positiv-ganz und $0<\alpha<1$ ist, definiert man

$$(4)\qquad f_k(z,x)=H^{-k}f(z,x)=\frac{1}{\Gamma(\alpha)}\int_0^z\left(\log\frac{z}{u}\right)^{\alpha-1}f_p(u,x)\frac{du}{z}$$
$$=\sum_{n=0}^{\infty}(n+1)^k P_n(x)z^n,$$

was auch für *negatives* $k=-\alpha(\alpha>0,\ p=0)$ noch brauchbar ist. Hierbei denken wir uns in der z-Ebene die Sperrlinien: $z=re^{\pm i\theta}(1\leqq r\leqq\infty)$; dabei möge aber doch die Integrationsvariable u in der gewöhnlichen Gauss-Ebene nur so angenommen sein, dass sie um 0, z, $e^{\pm i\theta}$ keine komplette Rotation leiste. Alsdann wird die erzeugende Funktion $f_k(z,x)$ im gesperrten z-Stern S überall eindeutig, also regulär bis auf $z=e^{\pm i\theta}$. Wir haben nur die Singularitäteigenschaft an diesen Stellen zu untersuchen.

3. Ist der erste Faktor unter dem Integralzeichen in (4)

$(\log z/u)^{\alpha-1}=[-\log(1-w)]^{\alpha-1}=w^{\alpha-1}E(w)$, wo $w=1-u/z$ ist,

gesetzt, so ist $E(w)$ regulär innerhalb des Kreises $|w|=1$, und deshalb folgende Entwicklung[1] gestattet:

$$(5)\qquad E(w)=1+c_1w+c_2w^2+\ldots\ldots+c_nw^n+\ldots\ldots$$
$$\text{mit}\quad c_n=O(n(\log n)^{2-\alpha});$$

somit konvergiert sie bei $0<\alpha<1$ für alle $|w|\leqq 1$ absolut und gleichmässig[2]. Andrerseits wird für $k=p-\alpha\leqq 0$ der zweite Faktor des Integranden in (4) nach (2) z. B. um den Punkt $\omega=e^{i\theta}(0<\theta<\pi)$:

$$(6)\qquad \frac{\Phi_p(z,x)}{(1-2xz+z^2)^{p+\frac{1}{2}}}=\frac{\mathfrak{P}(z,x)}{(1-\zeta)^{p+\frac{1}{2}}},\quad(\zeta=\omega^{-1}z),$$

wobei der rechts stehende Zähler

$$(7)\qquad \mathfrak{P}(z,x)=\sum_{m=0}^{\infty}a_m(1-\zeta)^m$$

als Radius des Konvergenzkreises den Wert $|\omega-\omega^{-1}|=2\sin\theta$ einnimmt. Wenn also $\pi/6<\theta<5\pi/6$ oder $|x|<\sqrt{3}/2$ ist, so liegt der Anfangspunkt $z=0$ zwar innerhalb des Konvergenzkreises und demgemäss konvergiert $\sum|a_m|$. In diesem Falle kann man das durch Einsetzung von (5), (6), (7) in (4) ausgebildete Cauchysche Produkt gliedweise integrieren:

---

1. Vgl. II, loc. cit. Dort genügt es nur die Bedingung $\alpha>0$ anzunehmen, ohne $\alpha<1$ zu beschränken. (Der Fall $\alpha=1$ ist trivial.) 2. Das unten aufgestellte Argument bleibt noch für den Fall $\alpha>1$ fast unveränderlich, falls man als untere Integrationsgrenze anstatt 0 nur $\epsilon e^{i\theta}$ nimmt und $\epsilon\to+0$ lässt.

$$(8)\qquad \begin{cases} f_k(z,\,x)=\sum_{\nu=0}^{\infty}\sum_{n=0}^{\nu}\dfrac{a_{\nu-n}c_n}{\Gamma(\alpha)}\displaystyle\int_0^z\left(\frac{z-u}{z}\right)^{n+\alpha-1}(1-\omega^{-1}u)^{\nu-n-p-\frac{1}{2}}\frac{du}{z} \\ \qquad\quad =\sum_{\nu=0}^{\infty}\mathfrak{f}_\nu(z). \end{cases}$$

Da ferner längs des Integrationswegs $u=\omega v$ $(0\leqq v\leqq|z|<1)$

$$(1-\omega^{-1}u)^{\nu-n-p-\frac{1}{2}}=\sum_{l=0}^{\infty}\binom{\nu-n-p-\frac{1}{2}}{l}(-v)^l$$

noch gleichmässig konvergiert, so möge die Integration in (8) durch diese Entwicklung wieder gliedweise durchgeführt werden. Also wird das Integral auf die hypergeometrische Reihe

$$F(p+n-\nu+\tfrac{1}{2},\ 1,\ \alpha+n+1,\ \zeta)/(n+\alpha)\qquad(\zeta=\omega^{-1}z)$$

zurückgeführt, deren analytische Fortsetzung um $z=\omega$ nach Barnes[1] bei $\alpha\neq g+\frac{1}{2}$ durch

$$(9)\qquad F(p+n-\nu+\tfrac{1}{2},\ 1,\ p-\alpha-\nu+\tfrac{3}{2},\ 1-\zeta)/(\nu-p+\alpha-\tfrac{1}{2})$$
$$+B(n+\alpha,\ p-\alpha-\nu+\tfrac{1}{2})(1-\zeta)^{\nu-p+\alpha-\frac{1}{2}}F(n+\alpha,\ 1,\ 1,\ 1-\zeta)$$

angegeben wird, wobei der Koeffizient eine Betafunktion ist. Werden diese Glieder für $n=0,\ 1,\ldots,\ \nu$ nach (8) zusammengesetzt, so ergibt sich

$$\mathfrak{f}_\nu(z)=\mathfrak{p}_\nu(1-\zeta)+(1-\zeta)^{\nu-k-\frac{1}{2}}\mathfrak{q}_\nu(1-\zeta),$$

wobei $\mathfrak{p}_\nu(Z)$, $\mathfrak{q}_\nu(Z)$ gewisse Potenzreihen mit Konvergenzradien $=1$ sind. Aber $\sum\mathfrak{p}_\nu$ sowie $\sum\mathfrak{q}_\nu Z^\nu$ konvergieren im Kreisbereich $\mathfrak{S}$: $|Z|\leqq 1-\varepsilon$ mit jedem beliebig klein bestimmten $\varepsilon(>0)$ gleichmässig. Es ist nämlich jede in (9) auftretende hypergeometrische Reihe (kurz $F_{n,\nu}(Z)$ genannt) in $\mathfrak{S}$ für alle n, ν gleichmässig beschränkt. Andrerseits sind die Reihen $\sum|a_m|$, sowie $\sum|c_n|$ für $0<\alpha<1$ wegen $c_n=O(1/n(\log n)^{2-\alpha})$, oder der ungefähren Form $\sum|c_n|/\sqrt{n+1}$ noch für $\alpha>1$ sämtlich konvergent, also alles $<K_1$.[2] Deshalb erhält man aus (8) und (9) für passend grosses ν_0, was aber von Z ganz frei ist,

$$\sum_{\nu=\nu_0}^{\infty}|\mathfrak{p}_\nu(Z)|\leqq\sum_{\nu=\nu_0}^{\infty}\sum_{n=0}^{\nu}\left|\frac{a_{\nu-n}c_nF_{n,\nu}(Z)}{\Gamma(\alpha)(\nu-p+\alpha-\frac{1}{2})}\right|<K_2\sum|a_m|\sum\frac{|c_n|}{\sqrt{n+1}}<K_3$$

bei $\alpha\neq g+\frac{1}{2}$. Bezüglich $\mathfrak{q}_\nu$ gilt nach (9) nach Summation

$$\mathfrak{q}_\nu(Z)=\frac{1}{\Gamma(\alpha)\cos\pi\alpha}\sum_{n=0}^{\nu}(-1)^n a_{\nu-n}c_nB(\alpha+n,\ \nu-n-p+\tfrac{1}{2})F_{n,\nu}(Z),$$

wobei die betreffende Betafunktion nach ihrem absoluten Betrage bei gegebenem $\nu(\geqq\nu_0)$ für $n=\nu$ ihren Höchstwert erreicht und tatsächlich $\geqq|\Gamma(\frac{1}{2}-p)|\nu^{p-\frac{1}{2}}$ wird. Ferner folgt aus der absolut-gleichmässigen Konvergenz von $\sum c_nw^n$ in $|w|\leqq 1-\varepsilon$ diejenige von

---

1. Z. B. s. Whittaker and Watson, Modern Analysis, 3rd Edition, p. 290—291.
2. Unten bezeichnen wir mit K_1, K_2,..... gewisse endliche positive Konstanten.

$$H^{-p+\frac{1}{2}}\sum c_n\bar{w}^n=\sum c_n(n+1)^{p-\frac{1}{2}}w^n.$$

Folglich gilt wieder in $\mathfrak{S}$ gleichmässig

$$\sum_{\nu=\nu_0}^{\infty}|q_\nu(Z)Z^\nu|<K_4\sum|c_n(n+1)^{p-\frac{1}{2}}Z^n|\ \sum|a_mZ^m|<K_5.$$

Also sind die gleichmässigen Konvergenzen von $\sum p_\nu$ und $\sum q_\nu Z^\nu$ vollständig bewiesen. Und demgemäss sieht man, dass in der Umgebung von $Z\equiv 1-z\omega^{-1}=0$

(10) $\quad f_k(z,x)=\psi(1-\zeta)+(1-\zeta)^{-k-\frac{1}{2}}\varphi(1-\zeta)\ \ (\zeta=z\omega^{-1})$ für $\alpha\neq g+\frac{1}{2}$

gilt, wobei ψ und φ um $\zeta=1$ regulär und $\varphi(0)\neq 0$ sind[1]. Bei $\alpha=g+\frac{1}{2}$, wo $g=0$ oder positiv-ganz ist, wird in (9) $\nu-p+g=h$ ganz oder 0. Hierauf soll man für positives oder verschwindendes h die folgende nach dem Barnesschen (l. c.) Lemma erhaltene Formel:

$$F(p+n-\nu+\tfrac{1}{2},\ 1,\ \alpha+n+1,\ \zeta)=B(n-h+g+\tfrac{1}{2},\ h+1)$$
$$\times(-(1-\zeta))^h\log(1-\zeta)^{-1}F(n+g+\tfrac{1}{2},\ 1,\ 1,\ 1-\zeta)+p_{n,\nu}(1-\zeta)$$

benutzen. Also erhält man in diesem Falle anstatt (10)

$$(11)\quad \begin{cases} f_k(z,x)=\psi(1-\zeta)+(1-\zeta)^{-p}\varphi(1-\zeta)+\log(1-\zeta)\eta(1-\zeta) \\ \qquad\qquad\qquad\qquad\qquad\qquad \text{für } k=p-\frac{1}{2}>0, \\ \text{oder}=\psi(1-\zeta)+(1-\zeta)^g\log(1-\zeta)\eta(1-\zeta)\quad(\zeta=z\omega^{-1}) \\ \qquad\qquad\qquad\qquad\qquad\qquad \text{für } k=-g-\frac{1}{2}<0, \end{cases}$$

wobei alle Funktionen ψ, φ, η um $\zeta=1$ regulär, und im oberen $\varphi(0)\neq 0$, sowie im unteren $\eta(0)\neq 0$ sind.

4. Für den Fall $(1>)|x|>\sqrt{3}/2$ scheitert der obige Beweisgang[2], weil dann $u=0$ ausserhalb des Konvergenzkreises der Potenzreihe $\mathfrak{P}(u,x)$ liegt. Ist aber nun

$$(12)\qquad \frac{\mathfrak{P}(u,x)}{(1-u\omega^{-1})^{p+\frac{1}{2}}}=\sum_{m=0}^{p}a_m(1-u\omega^{-1})^{m-p-\frac{1}{2}}+\sqrt{1-u\omega^{-1}}G(u)$$

gesetzt, so wird das Integral der ersten Summe auf der rechten Seite

$$(13)\qquad \frac{1}{\Gamma(\alpha)}\int_0^z\left(\log\frac{z}{u}\right)^{\alpha-1}\sum_{m=0}^{p}a_m(1-u\omega^{-1})^{m-p-\frac{1}{2}}\frac{du}{z}$$
$$=\frac{\varphi_0(1-z\omega^{-1})}{(1-z\omega^{-1})^{k+\frac{1}{2}}}+\psi_0(1-z\omega^{-1})\qquad \text{für } \alpha\neq g+\tfrac{1}{2},$$

ebenso wie in Absatz 3 gezeigt wurde. Also hat man nur das zweite Glied in (12) zu überlegen. Die Funktion $G(u)$ ist im Bereich $\mathfrak{S}$: $|1-u\omega^{-1}|\leqq\rho_1<r=2\sin\theta\leqq 1$ regulär und ihre Taylorsche Reihe

$$G(u)=\sum_{m=0}^{\infty}a'_m(1-u\omega^{-1})^m\qquad (a'_m=\text{voriges } a_{m+p+1})$$

---

1. Offenbar besteht (10) auch für $k=0$, wie aus $f_0(z,x)$ schon hervorgeht. 2. Das folgende Argument ist etwas umständlich. Ich versuchte jedoch vergebens diesen Fall aus dem obigen durch die Betrachtung der analytischen Fortsetzung in Bezug auf x abzuleiten.

konvergiert dort gleichmässig. Andrerseits gestattet sie die Entwicklung

$$G(u)=\sum_{m=0}^{\infty} b_m(u\omega^{-1})^m \qquad \text{für } |u|<1.$$

Es seien[1]

(14) $$z=\omega(1-\rho),\ z_1=\omega(1-\rho_1),\ z_0=\omega(1-\rho_0),\ u=\omega(1-v)$$
$$\text{mit } 0\leqq\rho\leqq\rho_1<\rho_0<r\leqq 1,$$

und das vorgelegte Integral werde folgendermassen geteilt[2]:

$$J=\frac{1}{\Gamma(a)}\int_0^z\left(\log\frac{z}{u}\right)^{\alpha-1}\sqrt{1-u\omega^{-1}}\,G(u)\frac{du}{z}=J_1+J_2$$

mit $$J_1=\frac{1}{\Gamma(a)}\int_0^{z_0}\sum_{n=0}^{\infty}c_n\left(\frac{z-u}{z}\right)^{n+\alpha-1}\sqrt{1-u\omega^{-1}}\sum_{m=0}^{\infty}b_m(u\omega^{-1})^m\frac{du}{z}$$

und $$J_2=\frac{1}{\Gamma(a)}\int_{z_0}^{z}\sum_{n=0}^{\infty}c_n\left(\frac{z-u}{z}\right)^{n+\alpha-1}\sum_{m=0}^{\infty}a'_m(1-u\omega^{-1})^{m+\frac{1}{2}}\frac{du}{z},$$

wobei jeder Integrationsweg geradeaus genommen ist. Wegen der absolut-gleichmässigen Konvergenzen der unter jedem Integral stehenden Summen ist auch gliedweise Integration ihres Cauchyschen Produktes zulässig. Also wird zuerst

(15) $$J_1=\sum_{\nu=0}^{\infty}\sum_{n=0}^{\nu}\frac{b_{\nu-n}c_n}{\Gamma(a)}\int_0^{z_0}\left(\frac{z-u}{z}\right)^{n+\alpha-1}\sqrt{1-u\omega^{-1}}(u\omega^{-1})^{\nu-n}\frac{du}{z},$$

worin das Integral durch Einsetzung von (14) zu

(16) $$J^{(1)}_{n,\nu}=\frac{1}{(1-\rho)^{n+\alpha}}\int_{\rho_0}^{1}(v-\rho)^{n+\alpha-1}\sqrt{v}\,(1-v)^{\nu-n}dv\equiv\frac{J_{n,\nu}}{(1-\rho)^{n+\alpha}}$$

wird. Die ausführliche Gestalt von $J_{n,\nu}$ kann unter Benutzung der binomischen Reihen-Entwicklungen wie folgt gewonnen werden:

$$J_{n,\nu}=\sum_{\lambda=0}^{\nu-1}(-1)^\lambda\binom{\nu-n}{\lambda}\left\{\sum_{l=0}^{\infty}\binom{n+\alpha-1}{l}(-\rho)^l/(n+\alpha-l+\lambda+\tfrac{1}{2})\right.$$
$$\left.-\rho_0^{n+\alpha+\lambda+\frac{1}{2}}\sum_{l=0}^{\infty}\binom{n+\alpha-1}{l}\left(\frac{-\rho}{\rho_0}\right)^l\Big/(n+\alpha-l+\lambda+\tfrac{1}{2})\right\}\quad\text{für } n\geqq 1,\ \nu\geqq 1;$$

oder durch teilweise Integration

$$J_{0,\nu}=\frac{1}{a}\sum_{\lambda=0}^{\nu-1}(-1)^\lambda\binom{\nu-1}{\lambda}\sum_{l=0}^{\infty}(-1)^l\binom{\alpha}{l}\left\{\frac{(2\nu+1)\rho^l-\rho_0^{\lambda+\alpha+\frac{3}{2}}(\rho/\rho_0)^l}{2(\lambda+\alpha-l)+3}\right.$$
$$\left.-\frac{\rho^l-\rho_0^{\lambda+\alpha+\frac{1}{2}}(\rho/\rho_0)^l}{2(\lambda+\alpha-l)+1}\right\}-\frac{1}{a}(1-\rho_0)^\nu\rho_0^{\alpha+\frac{1}{2}}\sum_{l=0}^{\infty}\binom{\alpha}{l}(-\rho/\rho_0)^l$$

für $\nu\geqq 1$;

---

1. Mit einer solchen Wahl geht noch keineswegs die allgemeine Gültigkeit verloren. Denn wenn analytische Funktionen längs eines Kontinuums gleich sind, so gilt dasselbe auch in dem ganzen gemeinen Definitionsbereich. 2. Für $a>1$ soll die untere Grenze der Integration als $+0$ genommen werden.

und $$J_{0,0}=\frac{1}{\alpha}\sum_{l=0}^{\infty}(-1)^l\binom{\alpha}{l}\frac{2(l-\alpha)}{2(l-\alpha)-1}\left\{\rho^l-\rho_0^{\alpha+\frac{1}{2}}(\rho/\rho_0)^l\right\};$$

wobei jede in Bezug auf l summierte unendliche Reihe absolut-gleichmässig in $\mathfrak{S}$: $(0\leqq|1-z\omega^{-1}|=\rho\leqq\rho_1<\rho_0<r\leqq 1)$ konvergiert. Also wird jedes $J_{n,\nu}$ und folglich auch jedes $J^{(1)}_{n,\nu}$ nichts weiter als eine Potenzreihe von $\rho(=1-z\omega^{-1})$, weil ρ_0 hier eine reine Konstante ist[1]. Demzufolge wird die innere Summe in (15)

$$\mathfrak{f}^{(1)}_{\nu}(Z)=\sum_{n=0}^{\nu}\frac{b_{\nu-n}c_n}{\Gamma(\alpha)}\mathfrak{p}^{(1)}_{n,\nu}(Z)\qquad(Z=1-z\omega^{-1})$$

und demnach auf eine bestimmte einzelne Potenzreihe von Z mit Konvergenzradius $=1$ reduziert. Ferner ist

$$J_1=\sum_{\nu=0}^{\infty}\mathfrak{f}^{(1)}_{\nu}(Z)$$

gleichmässig in $\mathfrak{S}$ konvergent. Denn aus (15) und (16) folgt

$$J_1=\sum_{\nu=0}^{\infty}\sum_{n=0}^{\nu}\frac{b_{\nu-n}c_n}{\Gamma(\alpha)}\cdot\frac{1}{(1-\rho)^{n+\alpha}}\int_{\rho_0}^{1}(v-\rho)^{n+\alpha-1}v\cdot\frac{(1-v)^{\nu-n}}{\sqrt{v}}dv.$$

In dem Integral sind die betrachteten Zahlen ganz reell und der letzte Faktor des Integranden $(1-v)^{\nu-n}/\sqrt{v}$ monoton abnehmend. Demnach erhält man mit Benutzung des zweiten Mittelwertsatzes der Integralrechnung

$$J^{(1)}_{n,\nu}=\frac{1}{(1-\rho)^{n+\alpha}}\cdot\frac{(1-\rho_0)^{\nu-n}}{\sqrt{\rho_0}}\int_{\rho_0}^{\xi}(v-\rho)^{n+\alpha-1}v\,dv\qquad(\rho_0<\xi(n,\nu)<1)$$
$$<\frac{(1-\rho_0)^{\nu-n}}{(n+\alpha)\sqrt{\rho_0}}\left(\frac{\xi-\rho}{1-\rho}\right)^{n+\alpha}\frac{(n+\alpha)\xi+\rho}{n+\alpha+1}<\frac{(1-\rho_0)^{\nu-n}}{(n+\alpha)\sqrt{\rho_0}}$$

wegen (14). Damit aber ergibt sich

$$\sum_{\nu=0}^{\infty}|\mathfrak{f}^{(1)}_{\nu}(Z)|<\sum_{\nu=0}^{\infty}\sum_{n=0}^{\nu}|b_{\nu-n}(1-\rho_0)^{\nu-n}|\cdot|c_n(n+\alpha)^{-1}|/\Gamma(\alpha)\sqrt{\rho_0}$$
$$=\sum|b_m(1-\rho_0)^m|\sum|c_n(n+\alpha)^{-1}|/\Gamma(\alpha)\sqrt{\rho_0}<K,\quad\text{w. z. b. w.}$$

Es bleibt noch

$$J_2=\sum_{\nu=0}^{\infty}\sum_{n=0}^{\nu}\frac{a'_{\nu-n}c_n}{\Gamma(\alpha)}\int_{z_0}^{z}\left(\frac{z-u}{z}\right)^{n+\alpha-1}(1-u\omega^{-1})^{\nu-n+\frac{1}{2}}\frac{du}{z}\tag{17}$$

zu berechnen. Das Integral wird auf Grund der bisherigen Substitution (14)

$$J^{(2)}_{n,\nu}=\int_{\rho}^{\rho_0}\left(\frac{v-\rho}{1-\rho}\right)^{n+\alpha-1}v^{\nu-n+\frac{1}{2}}\frac{dv}{1-\rho},\tag{18}$$

was sich wieder durch die bisherige Reihen-Entwicklung in

---

1. Im obigen wurde $\alpha\neq g+\frac{1}{2}$ angenommen. Sonst tritt entsprechend v^{-1} die Konstante $\log 1/\rho_0$ auf, was aber keinen wesentlichen Unterschied bietet.

$$\rho_0^{\alpha+\nu-l+\frac{1}{2}}(1-\rho)^{-n-\alpha}\sum_{l=0}^{\infty}\binom{n+\alpha-1}{l}(-\rho)^l/(\alpha+\nu-l+\tfrac{1}{2})$$
$$-\rho^{\alpha+\nu+\frac{1}{2}}(1-\rho)^{-n-\alpha}\sum_{l=0}^{\infty}(-1)^l\binom{n+\alpha-1}{l}/(\alpha+\nu-l+\tfrac{1}{2}) \quad \text{für } \alpha\neq g+\tfrac{1}{2}$$

verwandelt. (Dabei gesellt sich für $\alpha=g+\frac{1}{2}$ das Glied $(-\rho)^{g+\nu+1}\times\log(\rho_0/\rho)$ bei $l=g+\nu+1$ anstatt desjenigen mit verschwindendem Nenner hinzu.) Folglich wird die innere Summe in (17) bei $\alpha\neq g+\frac{1}{2}$

$$\mathfrak{f}_\nu^{(2)}(Z)=\sum_{n=0}^{\nu}\frac{a'_{\nu-n}c_n}{\Gamma(\alpha)}\left\{\mathfrak{p}_{n,\nu}^{(2)}(Z)+Z^{\alpha+\frac{1}{2}}\mathfrak{q}_{n,\nu}^{(2)}(Z)\right\} \qquad (Z=1-z\omega^{-1}).$$

(Dabei soll für $\alpha=g+\frac{1}{2}$ das zweite Glied durch $Z^{g+1}(\log Z^{-1})\ \mathfrak{q}_{n,\nu}^{(2)}(Z)$ ersetzt werden). Also wird $\mathfrak{f}_\nu^{(2)}(Z)$ eine Summe zweier Potenzreihen von Z, die zweite jedoch hierbei multipliziert mit $Z^{\alpha+\frac{1}{2}}$; dabei ist jeder Konvergenzradius $r=2\sin\theta>0$. Ferner ist

$$J_2=\sum_{\nu=0}^{\infty}\mathfrak{f}_\nu^{(2)}(Z)$$

wieder in $\mathfrak{S}$ gleichmässig konvergent. Denn da nach (17) und (18)

$$J_2=\sum_{\nu=0}^{\infty}\sum_{n=0}^{\nu}\frac{a'_{\nu-n}c_n}{\Gamma(\alpha)}\int_\rho^{\rho_0}\left(\frac{v-\rho}{1-\rho}\right)^{n+\alpha-1}v^{\nu-n+\frac{1}{2}}\frac{dv}{1-\rho}$$

ist, worin nun $v^{\nu-n+\frac{1}{2}}$ monoton zunehmend ist, so gilt

$$J_{n,\nu}^{(2)}=\rho_0^{\nu-n+\frac{1}{2}}\int_\eta^{\rho_0}\left(\frac{v-\rho}{1-\rho}\right)^{n+\alpha-1}\frac{dv}{1-\rho} \qquad (\rho<\eta(n,\nu)<\rho_0)$$
$$<\frac{\rho_0^{\nu-n}}{n+\alpha}\left(\frac{\rho_0-\rho}{1-\rho}\right)^{n+\alpha}<\frac{\rho_0^{\nu-n}}{n+\alpha}$$

wegen (14). Daraus aber folgt wohl

$$\sum_{\nu=0}^{\infty}|\mathfrak{f}_\nu^{(2)}(Z)|<\sum_{\nu=0}^{\infty}\sum_{n=0}^{\nu}|a'_{\nu-n}\rho_0^{\nu-n}|\cdot|c_n(n+\alpha)^{-1}|/\Gamma(\alpha)$$
$$=\sum|a'_m\rho_0^m|\sum|c_n(n+\alpha)^{-1}|/\Gamma(\alpha)<K, \qquad \text{w. z. b. w.}$$

Vermöge der gleichmässigen Konvergenz jeder der beiden Summen J_1 und J_2 in $\mathfrak{S}$ erhält man schliesslich für $\alpha\neq g+\frac{1}{2}$

(19) $\qquad J_1=\psi_1(1-z\omega^{-1}), \quad J_2=\psi_2(1-z\omega^{-1})+(1-z\omega^{-1})^{\alpha+\frac{1}{2}}\ \varphi_2(1-z\omega^{-1}),$

wobei ψ_1, ψ_2, φ_2 je Potenzreihen mit Konvergenzradius $r>0$ sind. Dabei soll die zweite Summe für $\alpha=g+\frac{1}{2}$ durch $(1-z\omega^{-1})^{g+1}\ (\log(1-z\omega^{-1}))\times\eta_2(1-z\omega^{-1})$ ersetzt werden. Werden (13) und (19) kombiniert, so ergibt sich wirklich das gesuchte Resultat (10) oder (11).

5. Man hat noch den Fall $x=-1$ zu erwägen[1]. In diesem Falle ist nach (3)

$$f_p(z,-1)=\chi_p(z)/(1+z)^{p+1} \qquad \text{für positiv-ganzes } p, \text{ und}$$

1. In diesem Falle kann dies mit $H^{-k}(1+z)^{-1}=\Sigma(n+1)^k(-z)^n$ betrachtet werden.

$$f_k(z,-1)=\frac{1}{\Gamma(\alpha)}\int_0^z\left(\log\frac{z}{u}\right)^{\alpha-1}\frac{\chi_p(u)}{(1+u)^{p+1}}\,\frac{du}{z}\quad\text{für}\quad k=p-\alpha\leqq 0,\ \alpha>0.$$

Dabei gilt nach (5), wenn $u/z=1-w$ gesetzt wird,

$$[\log(z/u)]^{\alpha-1}/w^{\alpha-1}=\sum c_n w^n\qquad\text{mit}\quad c_n=O(1/n(\log n)^{2-\alpha}),$$

was in $|w|<1$ gleichmässig konvergiert. Andrerseits ist $\chi_p(u)$ ein Polynom des $(p-1)$-ten Grades, und deshalb

$$\chi_p(u)/(1+u)^{p+1}=\sum_{m=0}^{p-1}a_m(1+u)^{m-p-1}.$$

Also wird

$$f_k(z,-1)=\frac{1}{\Gamma(\alpha)}\sum_{m=0}^{p-1}a_m\sum_{n=0}^{\infty}c_n\int_0^1 w^{n+\alpha-1}[1+z(1-w)]^{m-p-1}dw,\quad(|z|<1).$$

Die innere Summe wird nach der Integration zu

$$I_m=\sum_{n=0}^{\infty}c_nF(p-m+1,\ 1,\ n+\alpha+1,\ -z)/(n+\alpha)$$

reduziert, worin sich der Summand für gebrochenes α nach Barnes (l. c.) um $z=-1$ in

$$c_n\{F(p-m+1,\ 1,\ p-\alpha-m-n+2,\ 1+z)/(m+n-p+\alpha-1)$$
$$+B(n+\alpha,\ p-\alpha-m-n+1)(1+z)^{m+n-p+\alpha-1}F(n+\alpha,\ 1,\ 1,\ 1+z)$$

verwandelt. Das Gleiche gilt noch für jedes nicht-ganze α mit $p=0$; nun tritt aber nur die $m=0$ entsprechende einzelne Summe I_0 allein auf, weil jetzt $f_0(u,-1)=1/(1+u)$ ist. Daher gilt im allgemeinen in der Umgebung von $z=-1$

$$f_k(z,-1)=\psi(1+z)+\varphi(1+z)/(1+z)^{k+1}\qquad(k>-1\ \text{oder}\ -1>k\neq\text{ganz})^1.\tag{20}$$

wobei ψ, φ um $z=-1$ regulär und $\varphi(0)\neq 0$ ist.

Für positiv-ganzes α mit $p=0$ sei $n+\alpha-1=h$ (positiv-ganz oder 0) gesetzt. Die betreffende hypergeometrische Reihe wird nun

$$F(1,\ 1,\ h+2,\ -z)=p(1+z)+(h+1)(1+z)^h z^{-(h+1)}\log(1+z).$$

Also ergibt sich bei negativ-ganzem $k=-\alpha$ anstatt (20)

$$f_{-\alpha}(z,-1)=\psi(1+z)+(1+z)^{\alpha-1}\log(1+z).\eta(1+z)\qquad(\alpha:\ \text{positiv-ganz}),\tag{21}$$

wobei ψ, η um $z=-1$ regulär und $\eta(0)\neq 0$ ist.

6. *Darbouxsche Methode.* Es sei der Konvergenzkreis der Potenzreihe

$$F(z)=\sum_{n=0}^{\infty}c_nz^n\tag{22}$$

der Einheitskreis, und an dessen Rand soll nur eine endliche Anzahl singulärer Stellen $z=\omega_r$ $(r=1,\ 2,\ldots\ldots,\ l)$ liegen, in deren Umgebung

1. Bei $k=p$ oder 0 folgt (20) unmittelbar aus (2) und (3).

(23) $F(z)=\xi^{-\alpha_r}\varphi_r(\xi)+\xi^{-\beta_r}\eta_r(\xi)\log 1/\xi+\psi_r(\xi) \qquad (\xi=1-z\omega_r^{-1})$

gilt[1], wobei jedes $a_r(\neq 0)$ nicht negativ-ganz und

$$\varphi_r(\xi)=\sum_{s=0}^{\infty}a_{r,s}\xi^s,\ \eta_r(\xi)=\sum_{s=0}^{\infty}b_{r,s}\xi^s,\ \text{(wenigstens } a_{r,0} \text{ oder } b_{r,0}\neq 0),$$

$$\psi_r(\xi)=\ldots\ldots,$$

jede Potenzreihe von ξ mit Konvergenzradius >0 ist. Die Funktion $F(z)$ mit ihrer analytischen Fortsetzung verhält sich also regulär in dem längs $z=\omega_r R$ $(1\leqq R\leqq\infty)$ für $r=1, 2,\ldots\ldots, l$ gesperrten Stern S bis auf $z=\omega_r$. Wir wollen unten den asymptotischen Wert von c_n abschätzen. Zu diesem Zwecke aber soll das folgende Lemma vorausgeschickt werden.

7. Es sei

$$(24)\qquad F(z)-\sum_{r=1}^{l}\sum_{s=0}^{m}(a_{r,s}\xi_r^{s-\alpha_r}+b_{r,s}\xi_r^{s-\beta_r}\log 1/\xi_r)\equiv F_m(z) \quad (\xi_r=1-z\omega_r^{-1}),$$

was im Bereich S regulär, und in jeden Teilbereich $|z|\leqq 1+\Delta\,(\Delta>0)$ für passendes m sogar beschränkt bleibt. Deswegen gilt nach Cauchy

$$F_m(z)=\sum_{n=0}^{\infty}c_{n,m}z^n \qquad \text{mit} \quad c_{n,m}=\frac{1}{2\pi i}\int_{\mathfrak{C}}\frac{F(t)}{t^{n+1}}dt.$$

Dabei bestehe der Integrationsweg $\mathfrak{C}$ aus folgenden Teilen:

1° dem um $z=0$ als Mittelpunkt mit dem Radius $1+\Delta$ beschriebenen Kreis C,

2° dem um $z=\omega_r$ als Mittelpunkt mit allmählich gegen 0 strebendem Radius ρ beschriebenen Kreis γ_r $(r=1, 2,\ldots\ldots, l)$,

3° den beiden Seiten der Strecke δ_r zwischen $(1+\rho)\omega_r$ und $(1+\Delta)\omega_r$ $(r=1, 2,\ldots\ldots, l)$. Unser Lemma lautet: *Wird für jede gegebene positive Zahl* Ω *irgendeine positive ganze Zahl* m *passend gross bestimmt, so gilt* $c_{n,m}\equiv o(n^{-\Omega})$ *für* $n\to+\infty$.

Für den Beweis hat man die längs der obigen Teilwege genommenen Integral-Werte nacheinander abzuschätzen:

1° Längs C folgt aus der Beschränktheit des $F_m(z)$

$$(i)=\left|\int_C\right|<\frac{1}{2\pi}\int_0^{2\pi}\frac{K d\theta}{(1+\Delta)^{n+1}}=o(n^{-\Omega}) \qquad \text{für} \quad n\to\infty.$$

2° Wenn die Integrationsvariable t eine komplette Rotation um $z=\omega_r$ leistet, so bleiben für $q\neq r$ beide $(1-t\omega_q^{-1})^{s-\alpha_q}$ sowie $(1-t\omega_q^{-1})^{s-\beta_q}\times$

---

1. Oder etwas allgemeiner ausgedrückt: Es sei um $z=\omega_r (r=1, 2,\ldots, l)$

$$F(z)=\sum_{q=0}^{Q(r)}\Phi_{q,r}(\xi)+\Psi_r(\xi) \quad \text{mit} \quad \Phi_{q,r}(\xi)=\sum_{p=0}^{P(q,r)}\varphi_{p,q,r}(\xi)\{\log 1/\xi\}^p/\xi^{\alpha_{p,q,r}} (\xi=1-z\omega_r^{-1}),$$

wobei $\alpha_{0,q,r}(\neq 0)$ nicht negativ-ganz und $Q(r)$, $P(q,r)$ positiv-ganz oder 0 ist, während $\varphi_{p,q,r}(\xi)$, $\Psi_r(\xi)$ je eine Taylorsche Potenzreihe von ξ mit Konvergenzradius >0 ist. Dann kann ein analoges Resultat ganz genau so wie im Text erhalten werden.

$\log(1-t\omega_r^{-1})^{-1}$ unverändert. Folglich genügt es längs γ_r nur den Beitrag aus

$$(25)\qquad F(t)-\sum_{s=0}^{m}(a_{r,s}\tau^{s-\alpha_r}+b_{r,s}\tau^{s-\beta_r}\log 1/\tau)\qquad(\tau=1-t\omega_r^{-1})$$
$$=\tau^{m+1-\alpha_r}p_{r,m}(\tau)+\tau^{m+1-\beta_r}(\log 1/\tau)q_{r,m}(\tau)+\psi_r(\tau)$$

zu überlegen, wobei sich $p_{r,m}$, $q_{r,m}$ sowie ψ_r dort regulär verhalten, und demnach der Beitrag aus dem letzten Glied zunichte wird. Sind ferner $\alpha_r=\lambda_r+i\mu_r$ und $\beta_r=\lambda_r'+i\mu_r'$, so werden auf γ_r

$$|(\rho e^{i\varphi})^{-\alpha_r}|=\rho^{-\lambda_r}e^{\varphi\mu_r}=O(\rho^{-\lambda_r})\text{ sowie }|(\rho e^{i\varphi})^{-\beta_r}|=O(\rho^{-\lambda_r'}).$$

Also folgt

$$(ii)=\left|\int_{\gamma_r}\right|<K\int_0^{2\pi}\rho^{m+2-\lambda}(1+\log 1/\delta)d\varphi/(1-\rho)^{n+1},$$

falls $\lambda=\mathrm{Max.}(\lambda_r,\lambda_r')$ ist; demzufolge gilt bei $\rho=(n+1)^{-1}$ für $n>n_0$

$$(ii)<Ke(n+1)^{-m-2+\lambda+\varepsilon}=o(n^{-\Omega}),\qquad\text{wenn } m>\Omega+\lambda-2 \text{ ist.}$$

3° Es sei auf dem von $t_r=(1+\rho)\omega_r$ an bis zu $T_r=(1+\Delta)\omega_r$ sich erstreckenden Weg ein Zwischenpunkt $\tau_r=(1+1/\sqrt{n+1}\,\rho)\omega_r$ genommen, wobei $\rho=(n+1)^{-1}$ für $n>n_0$ ist, und demnach der ganze Weg δ_r in zwei Teilwege $\delta'_r(t_r,\tau_r)$ und $\delta''_r(\tau_r,T_r)$ geteilt wird. Wird der Hin- und Rückweg zusammengesetzt, so mögen hier wieder nur die in (25) rechts stehenden zwei ersten Glieder anstatt $F_m(t)$ genommen werden. Die Beiträge aus dem ersten Glied sind:

$$(iii)_1\leqq\left|\frac{1}{2\pi}\int_{\delta'_r}(1-t\omega_r^{-1})^{n+1-\lambda_r}t^{-n-1}p_{r,m}(t)dt\right|\cdot(1+e^{-2\pi\mu_r})$$
$$<K\sqrt{n+1}^{\lambda-m-2}e^{-1}=o(n^{-\Omega})\text{ für } m>2\Omega+\lambda-2, \text{ und}$$
$$(iii)_2<\frac{1}{2\pi}\int_{\delta''_r}\frac{\Delta^{m+1-\lambda}|p_{r,m}(t)dt|}{(1+1/\sqrt{n+1})^{n+1}}(1+e^{-2\pi\mu_r})<Ke^{-\sqrt{n}}=o(n^{-\Omega}),$$

während jene aus dem Glied mit Logarithmus:

$$(iii)_3<K\int_{\delta'_r}\sqrt{n+1}^{\lambda-m-1}\left\{(1+e^{-2\pi\mu'_r})\log(n+1)+2\pi\right\}|t^{-n-1}dt|$$
$$<K\sqrt{n+1}^{\lambda-m-2+\varepsilon}e^{-1}=o(n^{-\Omega})\quad\text{für } m>2\Omega+\lambda-2, \text{ sowie}$$
$$(iii)_4=\left|\int_{\delta''_r}\right|<Kn^{\varepsilon}e^{-\sqrt{n}}=o(n^{-\Omega})$$

hinzukommen. Werden alle diese Beiträge zusammengefasst, so ergibt sich $c_{m,n}=o(n^{-\Omega})$ für $m>2\Omega+\lambda$, w. z. b. w.

8. *Beweis der Darbouxschen Methode.* Man hat nach (22),(23),(24)

$$F(z)=\sum_{n=0}^{\infty}c_nz^n=\sum_{r=1}^{l}\sum_{s=0}^{m}\left\{a_{r,s}\xi_r^{s-\alpha_r}+b_{r,s}\xi_r^{s-\beta_r}\log 1/\xi_r\right\}+F_m(z)\qquad(\xi_r=1-z\omega_r^{-1}),$$

und so gilt vermöge des vorigen Lemmas

$$c_n=\sum_{r=1}^{l}\sum_{s=0}^{m}\left\{a_{r,s}A_n^{\alpha_r-s-1}+b_{r,s}B_n^{\beta_r-s-1}\right\}\omega_r^{-n}+o(n^{-\Omega}),$$

wobei $A_n^\delta=(\delta+1)(\delta+2)\ldots\ldots(\delta+n)/\lfloor n = O(n^{\Re\delta})$ wie üblich, und

$B_n^\delta=A_n^\delta(\log n)\{1+O(1/\log n)\}$ für nicht negativ-ganzes δ,

oder $=(-1)^{1-\delta}\Gamma(-\delta)n^\delta\{1+O(1/\log n)\}$ für negativ-ganzes δ

nach den Narumi-Hamyschen asymptotischen Formeln sind. Also ergibt sich für $n\to+\infty$ bei bestimmtem m

$$(26)\qquad c_n\cong\sum_{r=1}^{l}\left\{a_{r,0}A_n^{\alpha_r-1}+b_{r,0}B_n^{\beta_r-1}\right\}\omega_r^{-n}\ \text{(wenigstens } a_{r,0}\text{ oder } b_{r,0}\neq 0).$$

Besonders wenn es unter $\alpha_1, \alpha_2,\ldots, \alpha_l$ nur ein solches α_M gibt, dass $\Re\alpha_M>$ jedes andere $\Re\alpha_r$ sowie alle $\Re\beta_r$ ist, so gilt nach (26)

$$(27)\qquad c_n\cong a_{M,0}\omega_M^{-n}A_n^{\alpha_M-1},\ \text{wobei}\ a_{M,0}=[F(z)(1-z\omega_M^{-1})^{\alpha_M}]_{z=\omega_M}$$

ist. Ebenso, wenn $\Re\beta_N>\Re\alpha_r$ und die anderen $\Re\beta_r$ ist, so gilt

$$(28)\qquad c_n\cong b_{N,0}\omega_N^{-n}B_n^{\beta_N-1}$$

$$\text{mit}\ b_{N,0}=[F(z)(1-z\omega_N^{-1})^{\beta_N}/\log(1-z\omega_N^{-1})^{-1}]_{z=\omega_N}.$$

Wenn weiter $\Re\alpha_M=\Re\alpha_N>$ alle anderen $\Re\alpha_r$, sowie $>$alle $\Re\beta_r$ sind, so gilt

$$(29)\qquad c_n\cong a_{M,0}\omega_M^{-n}A_n^{\alpha_M-1}+a_{N,0}\omega_N^{-n}A_n^{\alpha_N-1}.$$

Ebenso gilt, wenn $\Re\beta_M=\Re\beta_N$ am grössten sind,

$$(30)\qquad c_n\cong b_{M,0}\omega_M^{-n}B_n^{\beta_M-1}+b_{N,0}\omega_N^{-n}B_n^{\beta_N-1}.$$

9. Jetzt sind wir imstande, die C_δ-Summabilität[1] der Reihe (1) zu beweisen. Sind

$$\sum_{n=0}^{n}(n+1)^k P_n(x)=\sigma_n,\qquad \sum_{m=0}^{n}A_{n-m}^{\delta-1}\sigma_m=\sigma_n^\delta$$

gesetzt, so haben wir

$$F(z)=\sum\sigma_n^\delta z^n=\sum\sigma_n z^n\sum A_n^{\delta-1}z^n=f_k(z,x)/(1-z)^{\delta+1}.$$

Diese Funktion hat den Einheitskreis als wahren Konvergenzkreis und die drei singulären Stellen $e^{i\theta}$, $e^{-i\theta}$ und 1, wenn $-1<x<1$ ist. Um die asymptotische Formel für σ_n^δ nach der Darbouxschen Methode zu bekommen, muss man nach dem Pol der höchsten Ordnung bei $k\geqq-1/2$, oder der Verzweigungs-Nullstelle der niedrigsten Ordnung bei $k<-1/2$ fragen. Zuerst[2] sei $f_k(1,x)\neq 0$. Dann wird für $\delta+1>k-\frac{1}{2}$ gemäss (10) oder (11) der gefragte Punkt $z=1$; folglich nach (27) bei $-1<x<1$

$$(31)\qquad \sigma_n^\delta\cong f_k(1,x)A_n^\delta,\ \text{d.h.}\ \sum(n+1)^k P_n(x)=f_k(1,x)\ (C,\ \delta>k-\tfrac{1}{2}).$$

Wenn hingegen $f_k(1,x)=0$, die Funktion $f_k(z,x)$ also wegen ihrer Regularität durch $(1-z)$ teilbar ist, so verhält sich $f_k(z,x)/(1-z)=\Psi_k(z,x)$ um $z=e^{\pm i\theta}$ singulär wie $f_k(z,x)$ selbst; denn man hat nur

---

1. Bei negativer Ordnung soll nur das gebrochene δ behandelt werden. 2. Für $k<0$ ist nach (4) sicherlich $f_k(1,x)>0$, wie θ auch immer sei.

jedes Glied in (10) oder (11) mit

$$(1-z)^{-1}=p(1-ze^{\mp i\theta})/(1-e^{\pm i\theta}) \quad (p(0)\neq 0)$$

zu multiplizieren, um die dortige Formel für $\Psi_k(z, x)$ zu erlangen. Daher erhält man für $\delta>k-\frac{1}{2}$, aber vorläufiges[1] $\delta<k+\frac{1}{2}$, vermöge (29) oder (30) $\sigma_n^\delta \cong A_n^{k-\frac{1}{2}}\{(1-e^{i\theta})^{-\delta}\Psi_k(e^{i\theta}, x)e^{-ni\theta}+(1-e^{-i\theta})^{-\delta}\Psi_k(e^{-i\theta}, x)e^{ni\theta}\}$, oder $B_n^{k-\frac{1}{2}} \times\{\ldots\ldots\}$, also $\sigma_n^\delta/A_n^\delta \cong 0$; d.h. $\sum(n+1)^k P_n(x)=o(C, \delta>k-\frac{1}{2})$.

Es sei nun $x=-1$. Die singulären Stellen der $F(z)$ werden nur ± 1. Falls ferner $f_k(1, -1)\neq 0$ ist, so sieht man vermöge (20) oder (21) nach (27), dass (31) noch für $\delta>k$ bei $x=-1$ gilt. Wenn schliesslich $f_k(1, -1)=0$ ist, wie bei $k=2, 4, 6,\ldots$ der Fall ist, so wird $f_k(z, -1)$ durch $(1-z)$ teilbar. Mit Rücksicht auf (20) oder (21) (aber nun durch $1-z$ dividiert) kann man sehen, dass für $\delta>k$, aber vorläufiges[1] $\delta<k+1$, unter Benutzung von (27) oder (28)

$$\sigma_n^\delta \cong a_{-1,0}A_n^k/2^\delta \text{ oder } b_{-1,0}B_n^k/2^\delta$$

und folglich $\sigma_n^\delta/A_n^\delta \cong 0$ gilt, also die C_δ-Summe$=0$ für jedes $\delta>k$ ist.

10. Es ist

$$\sum P_n(x)z^n=\frac{1}{\sqrt{1-2xz+z^2}}=\frac{1}{\sqrt{(1-ze^{-i\theta})(1-ze^{i\theta})}} \quad (x=\cos\theta).$$

Also gilt für $0<\theta<\pi$

$$F(z)\equiv\sum P_n(x)z^n=\frac{1}{\sqrt{(1-ze^{-i\theta})(1-e^{2i\theta})}}+\frac{1}{\sqrt{(1-ze^{i\theta})(1-e^{-2i\theta})}};$$

und daher erhält man nach (29), wie Darboux schon gezeigt hat,

$$P_n(x)\cong A_n^{-\frac{1}{2}}\left\{\frac{e^{-ni\theta}}{\sqrt{1-e^{2i\theta}}}+\frac{e^{ni\theta}}{\sqrt{1-e^{-2i\theta}}}\right\}$$

$$=\sqrt{\frac{2}{n\pi\sin\theta}}\cdot\cos\left\{(n+\tfrac{1}{2})\theta-\frac{\pi}{4}\right\},$$

was der sog. Laplacesche asymptotische Wert für $P_n(\cos\theta)$ ist, und in meinen früheren Arbeiten I, II (loc. cit.) oft zitiert wurde.

Auf Grund der obigen Laplaceschen Formel gilt $(n+1)^k P_n(x)=O(n^{k-\frac{1}{2}})$, und daraus folgt unmittelbar für $k>-\frac{1}{2}$ infolge des bekannten schönen Satzes von Dienes, dass unsere Reihe $\sum(n+1)^k P_n(x)$ wohl C_δ-summierbar ist. Aber jener Beweis scheitert für $k\leqq-\frac{1}{2}$, während der vorgelegte Beweis mit Hilfe der Darbouxschen Methode ganz allgemein durchgeführt worden ist, und sogar die gleichmässige C_δ-Summierbarkeit, wenn auch in etwas umständlicherer Weise, eventuell beweisbar bleibt.

---

1. Vermöge des sog. Konsistenzsatzes, der bei $\delta>-1$ von Chapman und bei $\delta<-1$ von Hausdorff herrührt, kann die vorläufige Beschränkung für δ aufgehoben werden.

On the Theory of Polynomials of Kernels

By **Tunezô Satô**

(Received December 30, 1935)

Let

$$\lambda_1, \lambda_2, \lambda_3, \ldots\ldots, \lambda_n, \ldots\ldots, \text{ where } |\lambda_i| \leqq |\lambda_{i+1}|,$$

and

$$\varphi_1, \varphi_2, \varphi_3, \ldots\ldots, \varphi_n, \ldots\ldots\ldots$$

be the system of characteristic constants and the corresponding normalized system of characteristic functions of the complete and symmetric kernel $K(x, y)$ respectively.

Corresponding to a polynomial of z

$$P(z) = c_1 z + c_2 z^2 + \ldots\ldots\ldots\ldots + c_m z^m,$$

where coefficients are all real, we consider the following polynomial of the kernel $K(x, y)$:

$$c_1 K + c_2 K^{(2)} + \ldots\ldots\ldots\ldots + c_m K^{(m)}.$$

Here every $K^{(i)}(x, y)$ means respectively the i-th iterated kernel of $K(x, y)$, and we denote this linear operator by $P(K)^{\binom{x}{y}}$

We see easily from the property of iterated kernels that

$$\varphi_i(x) = \lambda_i^m \int_a^b K^{(m)}(x, t) \cdot \varphi_i(t) dt;$$

and moreover

$$\varphi_i(x) = \mu_i \int_a^b P(K)^{\binom{x}{t}} \varphi_i(t) dt,$$

where $$\mu_i = \frac{1}{P\left(\frac{1}{\lambda_i}\right)} \qquad i = 1, 2, 3, \ldots\ldots\ldots\ldots,$$

Now we begin with the following

Theorem 1. *When the polynomial of* z, $P(z)$, *is* $\geqq 0$ *for* $|z| \leqq \frac{1}{|\lambda_1|}$, *the polynomial of the kernel* $K(x, y)$, $P(K)^{\binom{x}{y}}$, *is a symmetric and positive definite kernel.*

Proof. If we write

$$K^{(s)}(w) = \int_a^b \int_a^b K^{(s)}(x, t) \omega(t) \omega(x) dt dx,$$

then for any continuous function $\omega(x)$ we have

$$K^{(s)}(\omega) = \sum_{\nu=1}^{\infty} \frac{C_\nu^2}{\lambda_\nu^s}, \quad C_\nu = (\omega, \varphi_\nu),$$

since it is well known that for the symmetric kernel $K(x, y)$

$$K^{(s)}(x, y)=\sum_{\nu=1}^{\infty}\frac{\varphi_\nu(x)\varphi_\nu(y)}{\lambda_\nu^s} \qquad (s\geqq 2),$$

where the series of the second member converges absolutely and uniformly over the square domain : $[a\leqq x\leqq b,\ a\leqq y\leqq b]$. Therefore

$$\begin{aligned}\int_a^b\int_a^b P(K)\binom{x}{t}\omega(t)\omega(x)dtdx &= \sum_{p=1}^{m} c_p K^{(p)}(\omega)\\ &= \sum_{p=1}^{m} c_p \sum_{\nu=1}^{\infty}\frac{C_\nu^2}{\lambda_\nu^p}\\ &= \sum_{\nu=1}^{\infty} C_\nu^2 \sum_{p=1}^{m}\frac{c_p}{\lambda_\nu^p}\\ &= \sum_{\nu=1}^{\infty} C_\nu^2 P\left(\frac{1}{\lambda_\nu}\right).\end{aligned}$$

And since, by hypothesis, $P\left(\frac{1}{\lambda_\nu}\right)\geqq 0$ for all ν's, we have for any continuous function $\omega(x)$

$$\int_a^b\int_a^b P(K)\binom{x}{t}\omega(t)\omega(x)dtdx\geqq 0.$$

But if for a certain function $\omega(x)$, which is not identically zero,

$$\int_a^b\int_a^b P(K)\binom{x}{t}\omega(t)\omega(x)dtdx=0,$$

then for an arbitrary value of x

$$\int_a^b P(K)\binom{x}{t}\omega(t)dt=0,$$

thus we have the result that for all elements of the complete system $\{\varphi_\nu(x)\}$ $(\omega, \varphi_\nu)=0$; this contradicts the completeness of the system $\{\varphi_\nu\}$. Hence we have proved our theorem.

Another theorem resulting from the above viz.

Theorem 2. *None of the equalities*

$$P\left(\frac{1}{\lambda_i}\right)=0, \quad (i=1, 2, 3,.....)$$

exist.

We begin with this observation :—Corresponding to a polynomial of z with the constant term, e. g.

$$P_m(z)=c_0+c_1z+c_2z^2+.....+c_mz^m,$$

we cannot define the polynomial of kernel $K(x, y)$, being parallel to the above stated definition of one which corresponds to a polynomial of z without the constant term.

Now if we take $P_m^*(K)\binom{x}{y}$ as such a polynomial of a kernel which corresponds to $P_m(z)$, we must define the polynomial of the kernel, corresponding to $zP_m(z)$, as

$$KP_m^*(K)\binom{x}{y} \quad \text{or} \quad P_m^*(K)K\binom{x}{y}.$$

Thus we obtain

$$(1) \qquad \varphi_i(x)=\frac{1}{\frac{1}{\lambda_i}P_m\left(\frac{1}{\lambda_i}\right)}\int_a^b KP_m^*(K)\binom{x}{t}\varphi_i(t)dt, \qquad (i=1, 2, 3, \ldots\ldots\ldots).$$

Hence from this result characteristic properties of the kernel $P_m^*(K)\binom{x}{y}$ follow.

If we put

$$(2) \qquad \psi_i(u)=\int_a^b P_m^*(K)\binom{u}{t}\varphi_i(t)dt, \quad (i=1, 2, 3, \ldots\ldots\ldots)$$

from (1)

$$\mu_i\varphi_i(x)=\int_a^b K(x, u)\psi_i(u)du,$$

where $$\mu_i=\frac{1}{\lambda_i}P_m\left(\frac{1}{\lambda_i}\right).$$

While by the expansion theory

$$\mu_i\varphi_i(x)=\sum_{\nu=1}^{\infty}\frac{d_{\nu i}}{\lambda_\nu}\varphi_\nu(x) \quad \text{and} \quad d_{\nu i}=(\psi_i, \varphi_\nu)$$
$$(\nu=1, 2, 3, \ldots\ldots\ldots).$$

Since the system $\{\varphi_\nu\}$ is normalized and orthogonal,

$$d_{\nu i}=\begin{cases}\lambda_i\mu_i & \text{for } \nu=i\\ 0 & \nu\neq i,\end{cases}$$

that is, $d_{ii}=P_m\left(\frac{1}{\lambda_i}\right)$ and $d_{\nu i}=(\psi_i, \varphi_\nu)=0$.

Therefore, when we use

$$\bar{\psi}_i=\psi_i/P_m\left(\frac{1}{\lambda_i}\right)$$

in place of ψ_i, then for one of the i's and for all ν's

$$(\bar{\psi}_i, \varphi_i)=1, \quad (\bar{\psi}_i, \varphi_\nu)=0,$$

and on account of the completeness

$$\bar{\psi}_i\equiv\varphi_i, \quad \text{for} \quad i=1, 2, 3, \ldots\ldots\ldots .$$

Hence we have $\psi_i=P_m\left(\frac{1}{\lambda_i}\right)\varphi_i$. Put this result into (2).

Then we have

$$(3) \qquad P_m\left(\frac{1}{\lambda_i}\right)\cdot\varphi_i(x)=\int_a^b P_m^*(K)\binom{x}{t}\varphi_i(t)dt.$$
$$(i=1, 2, 3, \ldots\ldots\ldots)$$

Now we consider the following symmetric function:

$$\chi(x, t)\equiv P_m^*(K)\binom{x}{t}-\sum_{p=1}^{m}c_pK^{(p)}(x, t).$$

By using (3)

$$\int_a^b \chi(x, t)\varphi_i(t)dt = \int_a^b P_m^*(K)\binom{x}{i}\varphi_i(t)dt - \sum_{p=1}^{m} c_p \int_a^b K^{(p)}(x, t)\varphi_i(t)dt$$

$$= \left\{ P_m\left(\frac{1}{\lambda_i}\right) - \sum_{p=1}^{m} c_p \left(\frac{1}{\lambda_i}\right)^p \right\} \varphi_i(x)$$

$$= c_0 \varphi_i(x),$$

that is,

$$\varphi_i(x) = \frac{1}{c_0} \int_a^b \chi(x, t)\varphi_i(t)dt$$

for all $i = 1, 2, 3, \ldots\ldots\ldots$

But in order that these equations may be true for the same constant c_0, the characteristic constant $1/c_0$ cannot have a finite value. Hence we have $c_0 = 0$.

In conclusion the author wishes to express his hearty thanks to Professor Toshizô Matsumoto for his kind encouragement and remarks during the study.

Vol. XIX, No. 2, Published Mar. 31, 1936

Price - - - - Yen 1.00

These Memoirs are on Sale at

MARUZEN COMPANY, LTD.
TOKYO, OSAKA, KYOTO, NAGOYA, YOKOHAMA,
FUKUOKA & SENDAI

昭和十一年三月二十五日印刷
昭和十一年三月三十一日發行

編纂兼發行者　京都帝國大學理學部

印刷者　須磨勘兵衛
京都市下京區北小路通新町西

印刷所　內外出版印刷株式會社
京都市下京區西洞院通七條南

賣捌所　丸善株式會社
東京、大阪、京都、名古屋、横濱、福岡、仙臺

CONTENTS

Anomalous Deflection of Seismic Rays in Volcanic Districts (Part III of the Geophysical Studies on the Volcano Aso).
By Kenzô Sassa 65
A View of the Structure of the "Muroto Typhoon"
By Tadao Namekawa and Shiichi Aoki 79
Über die Legendresche Reihe $\sum(n+1)^k P_n(x)$
Von Yoshikatsu Watanabe 93
On the Theory of Polynomials of Kernels
By Tunezô Satô 105